Calving processes and the dynamics of calving glaciers

Douglas I. Benn [a,b,*], Charles R. Warren [a], Ruth H. Mottram [a]

[a] *School of Geography and Geosciences, University of St Andrews, KY16 9AL, UK*
[b] *The University Centre in Svalbard, PO Box 156, N-9171 Longyearbyen, Norway*

Abstract

Calving of icebergs is an important component of mass loss from the polar ice sheets and glaciers in many parts of the world. Calving rates can increase dramatically in response to increases in velocity and/or retreat of the glacier margin, with important implications for sea level change. Despite their importance, calving and related dynamic processes are poorly represented in the current generation of ice sheet models. This is largely because understanding the 'calving problem' involves several other long-standing problems in glaciology, combined with the difficulties and dangers of field data collection. In this paper, we systematically review different aspects of the calving problem, and outline a new framework for representing calving processes in ice sheet models. We define a hierarchy of calving processes, to distinguish those that exert a fundamental control on the position of the ice margin from more localised processes responsible for individual calving events. The first-order control on calving is the strain rate arising from spatial variations in velocity (particularly sliding speed), which determines the location and depth of surface crevasses. Superimposed on this first-order process are second-order processes that can further erode the ice margin. These include: fracture propagation in response to local stress imbalances in the immediate vicinity of the glacier front; undercutting of the glacier terminus by melting at or below the waterline; and bending at the junction between grounded and buoyant parts of an ice tongue. Calving of projecting, submerged 'ice feet' can be regarded as a third-order process, because it is paced by first- or second-order calving above the waterline.

First-order calving can be represented in glacier models using a calving criterion based on crevasse depth, which is a function of longitudinal strain rate. Modelling changes in terminus position and calving rates thus reduces to the problem of determining the ice geometry and velocity distribution. Realistic solutions to the problem of modelling ice flow therefore depend critically on an appropriate choice of sliding law. Models that assume that basal velocities are controlled by basal drag can replicate much of the observed behaviour of calving glaciers with grounded termini, but an important limitation is that they cannot be used to model floating glacier termini or ice shelves. Alternative sliding laws that parameterise drag from the glacier margins provide more flexible and robust ways of representing calving in ice sheet models. Such models can explain a remarkable range of observed phenomena within a simple, unifying framework, including: downglacier increases in velocity and strain rates where basal and/or lateral drag diminishes; flow acceleration in response to thinning through time; the tendency for glaciers to stabilise at 'pinning points' in relatively shallow water or fjord narrowings; the constraints on ice shelf stability; and the contrasts in calving rates between tidewater and freshwater calving glaciers. Many unresolved issues remain, however, including the role played by the removal of backstress in the acceleration of retreating calving glaciers, and the controls on melting at and below the waterline.
© 2007 Elsevier B.V. All rights reserved.

Keywords: calving; crevasses; glacier velocity; glacier dynamics; ice sheet models

---

* Corresponding author. The University Centre in Svalbard, PO Box 156, N-9171 Longyearbyen, Norway.
 E-mail address: doug.benn@unis.no (D.I. Benn).

1. Introduction

Calving, or the mechanical loss of ice from glaciers and ice shelves, is an important component of the mass budget of many glacier systems worldwide. It accounts for most of the mass loss from the Antarctic Ice Sheet, and contributes substantially to losses from the Greenland Ice Sheet and many other glaciers and ice caps (Jacobs et al., 1992; Hagen et al., 2003; Rignot and Kanagaratnam, 2006). During the Pleistocene, large portions of successive Laurentide, Fennoscandian, British–Irish, Patagonian and other ice sheets terminated in the sea and/or large proglacial lakes, and calving processes appear to have exerted a strong influence on their patterns of growth and retreat (Cutler et al., 2001; Hughes, 2002; Hulton et al., 2002; Zweck and Huybrechts, 2003; Mangerud et al., 2004; Siegert and Dowdeswell, 2004; Stokes and Clark, 2004). The past and present extent of calving glaciers is of particular importance because their dynamic behavior is at least partially de-coupled from climate, with factors other than variations in the equilibrium line altitude being major controls on the position, and rate of advance or retreat, of calving termini (Mercer, 1961; Mann, 1986; Meier and Post, 1987; Alley, 1991; Powell, 1991; Warren, 1991, 1992; Fischer and Powell, 1998; Vieli et al., 2001; Elsberg et al., 2003; Nick and Oerlemans, 2006; Nick et al., in press). Calving glaciers can undergo very rapid retreat following an initial climate signal (Post, 1975; Meier, 1997), and thereby have the potential to contribute disproportionately to global sea level rise (Meier and Post, 1987; Rignot et al., 2003). An understanding of calving processes is therefore crucial for the accurate prediction of cryospheric response to future climate forcing, and consequent sea level change. The effect of calving events on the ocean system is equally important. Large icebergs have a cooling effect on the oceans through latent and sensible heat exchanges, so changes in iceberg fluxes and routing can influence the larger climate system (Kenneally and Hughes, 2006). Layers of ice-rafted debris in marine sediment cores record major calving events (e.g. 'Heinrich Events'), and an understanding of calving processes is required if the complex web of climatic, oceanographic and glaciological causes and effects of such events is to be unravelled (Clarke et al., 1999). Finally, for mountain glaciers, the onset of calving at formerly land-based termini transforms their dynamics and climatic sensitivity (Kirkbride, 1993; Chinn, 1996), sometimes with hazardous results (Yamada, 1998; Benn et al., 2001). In sum, then, from the perspectives of Quaternary science, glaciology and global environmental change, and also in terms of societal relevance, there is a clear need to understand calving and associated dynamic processes.

Understanding the processes that control calving rates, however, has long been a major unsolved problem in glaciology. Although several empirical calving relations have been proposed, all are tied to specific datasets and/or regions, and a single, all-embracing 'calving law' has proved elusive (Meier and Post, 1987; Reeh, 1994; Van der Veen, 2002). In common with many glaciological enigmas, the obstinacy of the calving problem is a consequence of its multivariate nature and its great variability in time and space, compounded by the difficulties and dangers of the research environment. In the case of calving, the problem is further compounded by the fact that involves a number of other long-standing problems, such as finding realistic but tractable ways of computing stresses in the vicinity of the grounding line ('the grounding line problem') and rates of basal motion ('the unresolved sliding problem'), in addition to dealing with poorly understood mechanisms of brittle failure in ice. Over the years, the calving problem has been addressed from several different angles, and a large and diverse literature has built up. Several key questions have been identified, including: (1) What is the relationship between calving and glacier dynamics? Can calving retreat trigger fast flow, or vice versa? (2) What accounts for variations in calving rates between different environments, particularly freshwater and marine glacier margins? (3) How can calving processes be adequately represented in numerical models of ice sheet evolution?

1.1. Relationship between glacier dynamics and calving processes

Recent thinning, acceleration and rapid retreat of calving glaciers in many parts of the world (Fig. 1) has fuelled an intense debate concerning the relationship between calving and glacier dynamics. A central issue is whether calving losses are the cause or the consequence of flow acceleration. One conception of the relationship sees calving as the 'master', with calving losses triggering a cascade of dynamic changes up-glacier, including flow acceleration (Hughes, 1986; Meier and Post, 1987; Meier, 1994; Hughes, 1996; Meier, 1997; Howat et al., 2005). According to this view, 'calving is the local driving process, and the ice dynamics changes in response to this driving' (Meier, 1997, p. 113). In contrast, another view of the relationship portrays calving as the 'slave' of glacier dynamics, responding more or less passively to changes in other parts of the system (Van der Veen, 1996; Venteris et al., 1997; Van der Veen, 2002). In this view, coupled dynamical and geometric changes to the glacier system drive increased calving fluxes, by causing the calving

front to retreat and increasing the rate at which ice is delivered to that point. Thus flow acceleration and thinning control calving activity, instead of *vice versa*. The fact that both concepts were developed using the Columbia Glacier dataset, by far the most comprehensive available, emphasizes the intricate nature of the problem.

Both conceptions have empirical support, with some studies pointing to calving as the 'master' (Theakstone, 1989; Motyka et al., 2003a; Joughin et al., 2004) and others providing evidence that changes in terminus dynamics and glacier thinning may precede increased calving (Fischer and Powell, 1998; Kirkbride and Warren, 1999). Statistical relationships representing both the 'slave' and 'master' concepts succeed in explaining a similar percentage of observational data, while hinting at diametrically opposite conclusions regarding the direction of causality.

1.2. Contrasts between tidewater and freshwater calving

Because most of the pioneering work on calving was carried out on Alaskan tidewater glaciers, notably at Columbia Glacier (Krimmel, 2001), calving in fresh-water received relatively little attention and was assumed to be indistinguishable; 'calving glacier' and 'tidewater glacier' were widely yet inaccurately used as synonyms. However, studies of glaciers calving into hydropower storage lakes suggested that calving rates in freshwater were lower than those in tidewater (Bindschadler, 1980; Funk and Röthlisberger, 1989; Hooke et al., 1989; Laumann and Wold, 1992) and that, as a consequence, freshwater calving glaciers may occupy an intermediate position on the 'climatic sensitivity' spectrum between non-calving and tidewater glaciers (Warren, 1991). Subsequent work in Patagonia, New Zealand, Alaska and Norway has shown that freshwater calving rates are consistently about an order of magnitude lower than tidewater rates in comparable settings (Warren et al., 1995a; Kennett et al., 1997; Rott et al., 1998; Stuefer, 1999; Warren, 1999; Skvarca et al., 2002; Motyka et al., 2003b; Warren and Kirkbride, 2003; Haresign, 2004). Such differences have been attributed to contrasts in water densities, upwelling rates (and associated turbulent heat transfer), subaqueous melt rates, frontal oversteepening and longitudinal strain rates (Funk and Röthlisberger, 1989; Warren et al.,

Fig. 1. A) Columbia Glacier, Alaska, June 2005. (W.T. Pfeffer, INSTAAR, University of Colorado at Boulder, USA. Image from the forthcoming book "Columbia Glacier at Mid-Retreat: The Opening of a New Landscape" to be published by American Geophysical Union. B) Ice front retreat, Columbia Glacier, 1978–2000. From Krimmel (2001).
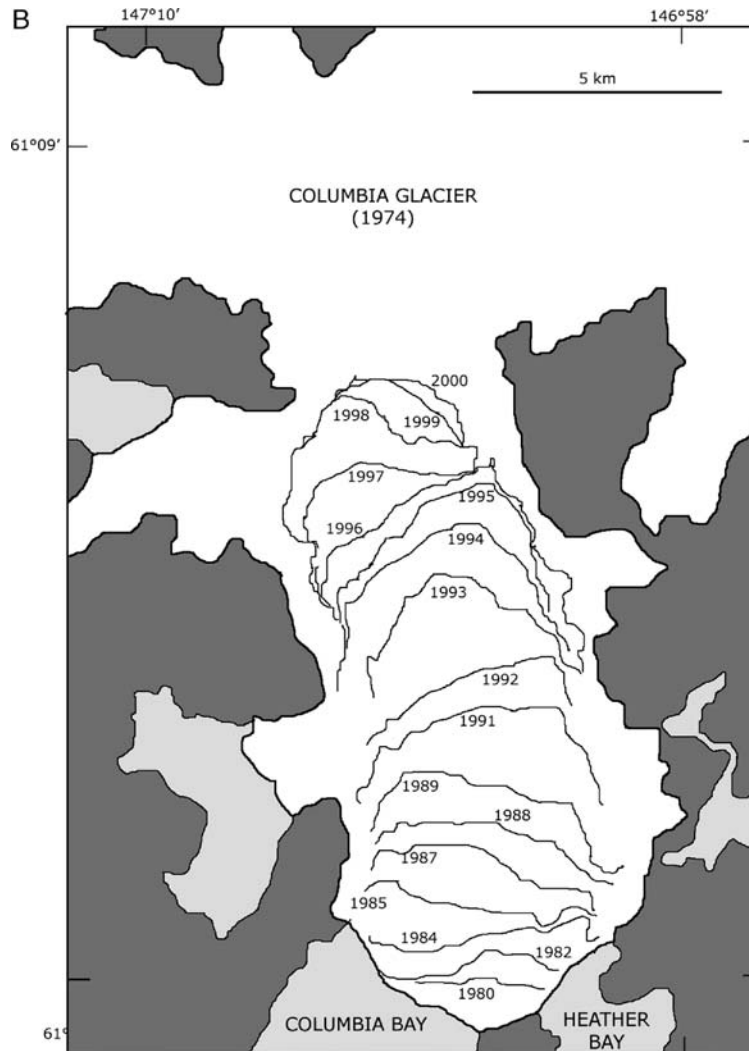
Fig. 1 (*continued*).

1995a; Van der Veen, 2002). The discovery of systematic differences between tidewater and freshwater calving is significant not only for understanding the dynamics of the many contemporary ice masses which calve into freshwater (e.g. in Alaska and Patagonia: Post and Mayo, 1971; Warren and Aniya, 1999) but also for interpreting the palaeoglaciological record of ice sheets which terminated in vast ice-contact lakes in Eurasia and North America (Teller and Kehew, 1994; Mangerud et al., 2004; Stokes and Clark, 2004).

1.3. Representation of calving in glacier models

The successful prediction of the response of ice sheets to climate change relies on the accurate parameterisation of mass losses at marine and lacustrine margins. In the current generation of ice sheet models, however, calving rates are determined using poorly-tested empirical functions with little or no physical basis. The choice of 'calving law' exerts a very strong influence on ice sheet sensitivity (Siegert and Dowdeswell, 1995), but to date only a few studies have tested model outputs against observations (e.g. Vieli et al., 2002; Nick and Oerlemans, 2006; Nick, 2006). The uncertainty surrounding appropriate 'calving laws' is compounded by the difficulty of incorporating realistic 'sliding laws' into ice sheet models (Benn et al., in press). Coupled dynamic and calving processes have the potential to transfer mass from glaciers and ice sheets to the oceans much more rapidly than surface melting, so the processes most likely to make a significant contribution to future sea-level rise are the very processes that are least well represented in current models.

There is therefore a clear need for a robust, flexible 'calving law', capable of being applied in a wide variety of settings, including marine and freshwater environments, and floating and grounded glacier margins. In addition, the relationships between calving and dynamic processes need to be more fully understood, and better represented in models.

The essence of the calving problem was summed up by Meier (1997, p.112), who stated that: 'iceberg calving is largely a problem in fracture mechanics coupled to ice dynamics'. In this paper, we address this two-fold nature of the calving problem, examining in turn the controls on (1) the formation and propagation of fractures in ice and the their role in calving processes, and (2) the velocity and dynamic behavior of water-terminating glaciers. A new model framework is then outlined, which incorporates a versatile 'calving law' based on a fracture criterion, an improved basal sliding function, and feedbacks between calving and dynamic processes. First, we review existing methods of representing calving losses in glacier models.

2. 'Calving laws'

2.1. Calving rate: Definition

Calving rate U_C is usually defined as the difference between ice velocity at the glacier terminus and glacier length change over time:

$$U_C = \overline{U}_T - \frac{dL}{dt} \tag{1}$$

where $\overline{U}_T$ is the vertically-averaged glacier velocity, L is the glacier length and t is time. Eq. (1) can also be expressed in terms of mass fluxes per unit width, including losses by melting:

$$Q_C - Q_M = H.\overline{U}_T - H.\frac{dL}{dx} \tag{1a}$$

where Q_C is calving flux and Q_M is the melt rate at the terminal ice cliff (Motyka et al., 2003a).

Two contrasting approaches have been taken to solving Eq. (1). In the first, calving rate is estimated from independent variables, and is then used in combination with ice velocity to predict changes in terminus position (e.g. Sikonia, 1982; Bindschadler and Rasmussen, 1983; Siegert and Dowdeswell, 2004), whereas the second approach uses ice velocity and changes in terminus position to determine calving losses (e.g. Van der Veen, 1996; Vieli et al., 2001; Van der Veen, 2002; Vieli et al., 2002). The advantages and disadvantages of these two approaches serve to illustrate many of the

paradoxes surrounding the calving problem, and are examined in turn in the following sections.

2.2. Calving rate functions

Several authors have sought relationships between calving rates and independent environmental variables such as water depth, ice velocity, and stretching rate. For a sample of 12 tidewater calving glaciers in Alaska, Brown et al. (1982) analysed several possible controlling variables, and found that calving speed showed a strong, linear relationship with water depth D_W at the terminus. Using a larger dataset ($n = 22$) from Alaska, Greenland and Svalbard, Pelto and Warren (1991) derived the following water depth–calving speed relationship:

$$U_C = 70 + 8.33\ D_W(\ ma^{-1}) \tag{2}$$

Funk and Röthlisberger (1989) found that for a sample of freshwater-calving glaciers, calving speeds were an order of magnitude less than those expected for tidewater glaciers. The contrast between tidewater and freshwater calving rates has been confirmed in numerous subsequent studies (e.g. Warren et al., 1995a; Warren and Kirkbride, 2003). For 21 freshwater-calving glaciers, the latter authors derived the relationship:

$$U_C = 17.4 + 2.3\ D_W(\ ma^{-1}) \tag{3}$$

A global data set compiled by Haresign (2004), however, shows that relationships between calving rate and water depth vary between regions (Fig. 2), and Van der Veen (1996, 2002) has shown that it can also change through time for a single glacier. For the Columbia Glacier, Sikonia (1982) found that although the water-depth law worked well for annually averaged data, it broke down for shorter time periods, with an r^2 value of
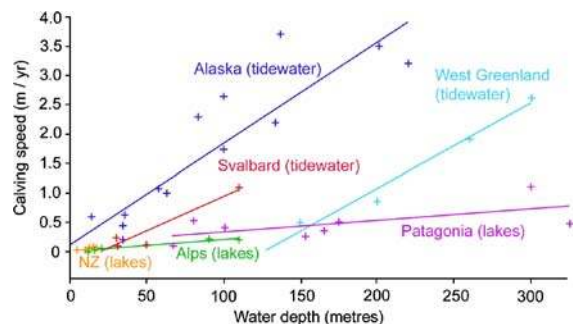
Fig. 2. Variation of calving rate with water depth for tidewater and freshwater calving glaciers in different regions. From Haresign (2004).

only 0.08. For calving rates averaged over c. 2 month intervals, he found an alternative function with $r^2 = 0.83$:

$$U_C = 1.092 \times 10^6 Q^{0.5689} H_O^{-2.175} \qquad (4)$$

where Q is the discharge of the nearby Knik River (a proxy for subglacial water flux), H_O is the height of the terminal ice cliff above buoyancy:

$$H_O = H_T - \frac{\rho'_W}{\rho_I} D_W \qquad (5)$$

ρ_I, ρ'_W are the densities of ice and the proglacial water body, respectively, and H_T is the ice thickness at the terminus. This interesting expression indicates that calving rates increase at times of high subglacial water flux, and when the glacier terminus approaches buoyancy, thus emphasising glacier dynamic rather than external environmental controls. The parameters in Eqs. (2)–(4) must be tuned to fit different data sets, limiting their value as general predictors of calving rate, or calving functions in ice sheet models. Additionally, Eq. (4) cannot be used for floating glacier tongues, because the predicted calving speeds tend toward infinity as H_O approaches zero. Nevertheless, Eqs. (2)–(4) are very useful as indicators of possible controls on calving processes. Any comprehensive theory of glacier calving must be able to explain the tendency for calving rate to increase with water depth, and the rate of increase to be greater for tidewater glaciers than for freshwater, as well as the influence of subglacial water and buoyancy on calving fluxes.

2.3. Controls on terminus position

Van der Veen (1996) inverted the calving problem, focusing on the factors that control the *position* of a calving terminus rather than those that might control the calving *rate*. Using a 17 yr series of data from Columbia Glacier, Van der Veen noted that the calving front tends to be located where H_O 50 m. If the glacier thins (either by melting or dynamic thinning), the calving front will retreat to a position where the height-above-buoyancy criterion is again satisfied. The height-above-buoyancy model, originally proposed by Sikonia (1982), was also found to apply at some Patagonian calving glaciers (Venteris, 1999). A modified version of the Van der Veen calving criterion was adopted by Vieli et al. (2000, 2001, 2002) in modelling studies of the advance and retreat of calving glaciers. Their model solves the equations for stress and velocity fields using finite-element software, and includes a water-pressure dependent sliding relation that scales sliding speed to ice thickness and depth of the glacier bed below sea level.

The position of the calving front is defined by a modified flotation criterion, replacing the fixed height above buoyancy H_O with a fraction q:

$$H_C = (1 + q) \frac{\rho'_W}{\rho_I} D_W \qquad (6)$$

A value of $q = 0.15$ yields $H_O = 50$ m for Columbia Glacier. The Vieli et al. model exhibits qualitatively similar behavior to some calving glaciers, including asymmetric responses to imposed mass balance cycles, with slow advance followed by rapid retreat (*cf*. Warren, 1992). It also performed well in modelling the observed retreat of Hansbreen, a tidewater glacier in Svalbard (Vieli et al., 2002).

An important shortcoming of the height-above-buoyancy model, however, is that it cannot allow for the formation of ice shelves, because the model 'cuts off' the glacier terminus before flotation is reached. As a result, the model cannot be used to predict the behavior of Antarctic glaciers or ice streams that flow into ice shelves, or to explore the evolution of marine ice sheets from floating ice. At a more fundamental level, the height-above-buoyancy model cannot explain why some glaciers can thin past the flotation thickness and form ice shelves before calving, nor can it be used to explain calving at termini which are far from flotation.

3. Fractures: Crevasse formation and propagation

All calving events are a consequence of the propagation of fractures (crevasses) in response to stress. Calving occurs when pre-existing or new fractures propagate sufficiently to isolate blocks from the main glacier mass, which then fall or float away from the terminus. Thus, the location, magnitude and timing of calving events are preconditioned by fracture propagation, and the position and form of calving margins reflects the distribution and orientation of former fractures. The key questions relevant to an understanding of calving processes are, therefore: (1) What criteria must be met for fractures to propagate through ice? (2) What controls the rate of fracture propagation? (3) What controls the depth (or length) of fractures? (4) What determines the orientation of fractures?

The issues will now be addressed in turn, to provide a basis for a systematic examination of calving processes.

3.1. Failure criteria

Sustained growth of fractures will occur when the stresses acting on suitably-oriented pre-existing cracks exceed some threshold. Three modes of fracturing can be

identified (Fig. 3). In Mode I, the walls of the fracture are pulled apart, and the fracture plane develops normal to the axis of maximum extension. In Mode II failure, the walls of the fracture remain in contact while the fracture develops along a shear plane and propagates in the direction of shearing. Mode III failure also involves development of fractures parallel to a shear plane, but fracture propagation is at right angles to the direction of shearing (tearing mode). Individual fracture events may involve two or all three modes simultaneously, called mixed mode fracture. Most studies of fracturing of glacier ice focus on Mode I failure, although recently some authors have considered other modes (Schulson and Hibler, 1991; Van der Veen, 1999a,b).

Failure criteria for ice have been established from both laboratory experiments and field data, although often with ambiguous or inconsistent results. Results from laboratory experiments are typically expressed in terms of the applied stress at point of failure (yield stress, in Pa) or the fracture toughness (Pa m$^{0.5}$). Tensile stresses on glaciers are difficult to measure directly, so failure criteria derived from field data are commonly expressed in terms of the threshold strain rate (m m^{-1} yr^{-1}) required for crevasse initiation. Conversion between yield stresses and threshold strain rates can be done by inverting Glen's flow law for ice:

$$\dot{\varepsilon}_{ij} = A\tau_e^{n-1}\tau_{ij} \tag{7}$$

to yield:

$$\tau_{ij} = A^{-1/n}\dot{\varepsilon}_e^{1/n-1}\dot{\varepsilon}_{ij} \tag{8}$$

where $\dot{\varepsilon}_{ij}$ and τ_{ij} are strain rate and stress components, $\dot{\varepsilon}_e$ and τ_e are the effective strain rate and effective stress, and A and n are the flow law parameters. In practice, the use of this approach is compromised because it relies on assumed values of A and n (which may differ widely for intact and damaged ice), and field data commonly do not allow full stresses to be calculated.

Observed threshold strain rates for the initiation of crevassing on glaciers span a wide range. For example,
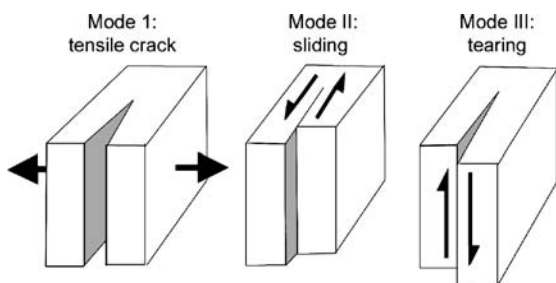

Fig. 3. Schematic diagram of the three basic modes of fracturing.

Meier (1958) derived values of around 0.01 yr^{-1} in Greenland, whilst on White Glacier, Canada, Hambrey and Muller (1978) recorded crevasses in areas with strain rates as low as 0.004 yr^{-1}, but not in areas with strain rates of 0.163 yr^{-1}. Vaughan's (1993) reanalysis of published threshold strain rates indicates yield stresses varying between 90 kPa and 320 kPa, a range that may reflect differences in ice rheology, crevasse spacing, and the influence of complex stress histories (*cf.* Kehle, 1964; Van der Veen, 1998a,b). Laboratory studies of failure criteria for ice have been conducted by Nixon and Schulson (1987), Fischer et al. (1995), Weber and Nixon (1996), Rist and Murrell (1994), Rist et al. (1996, 1999) and others. A useful recent summary has been provided by Petrovic (2003). These studies indicate that the tensile strength varies between 80 and 140 kPa at 0 °C and between 100 and 130 kPa at −50 °C, and that loading rate appears to be much more important than temperature in determining the stress at which failure occurs. Additionally, the presence of impurities may bring the tensile ice strength down to less than 10 kPa for temperatures between 0° and −50 °C. The compressive fracture strength is considerably higher but also much more variable at 5 MPa to 30 MPa between 0 °C and −40 °C. Unfortunately, few of these studies have used glacier ice, so their applicability to glaciers and ice sheets is uncertain.

3.2. Fracture propagation rates

In some circumstances, calving rates may be controlled by the rate of fracture propagation through ice (e.g. Iken, 1977; Kenneally and Hughes, 2002; Pralong and Funk, 2005). Following Evans (1984), Kenneally and Hughes (2002) used creep fracture theory to obtain a formula for crack propagation rates:

$$\frac{\partial d}{\partial t} = \frac{1}{\varepsilon_f}\left(\frac{\sigma_n n}{(n+1)A}\right)^n (H-d)^{n/(n+1)} d_c^{n/(n+1)} \tag{9}$$

where d is crack depth, ε_f is the threshold fracture strain rate, d_c is a constant related to ice ductility, H is ice thickness, and σ_n is the net tensile stress normal to the plane of the crack. This function was used in conjunction with assumed crack spacing to derive calving rates for specified glacier geometries. An alternative approach has been developed by Pralong et al. (2003) and Pralong and Funk (2005) using continuum damage mechanics. Rather than focusing on individual cracks, this approach models the propagation of damaged regions, which are sensitive to the evolving geometry of the system. The approach was applied to simulate the failure of blocks of ice on hanging Alpine glaciers, and produced a good fit to observed

geometric evolution and block acceleration prior to failure.

3.3. Crevasse depths

An alternative to modelling crevasse propagation rates is to calculate theoretical crevasse depths for given stress conditions, and to use these as a basis for determining the location of calving margins (Benn et al., in press; Section 4.6). This approach is based on the idea that crevasses will penetrate to a depth where the forces encouraging crack propagation are exactly balanced by those opposing it. Nye (1957) derived a function for calculating the equilibrium depth of a Mode I surface fracture by assuming that it will extend to a depth where the tensile strain rate (which tends to open the fracture) exactly balances the creep closure rate resulting from ice overburden pressure:

$$d = \frac{2}{\rho_I g} \left(\frac{\dot{\varepsilon}}{A} \right)^{\frac{1}{n}} \tag{10}$$

(g is gravitational acceleration and $\dot{\varepsilon}$ is the tensile strain rate). In Eq. (10), fracture growth is assumed to occur under any tensile stress, however small, although a yield criterion can be incorporated by replacing $\dot{\varepsilon}$ with $\dot{\varepsilon}*$, or $\dot{\varepsilon}$ minus the threshold strain rate required for crevasse initiation. This formulation neglects the effects of stress concentrations at the tip of the crack, so it is most applicable for the case of closely-spaced crevasses where stress concentration effects are reduced by the presence of nearby fractures.

The effect of stress concentrations on equilibrium crevasse depths was first examined by Weertman (1973) and Smith (1976, 1978), who derived approximate equations for the penetration depth of isolated crevasses. More rigorous work was conducted by Rist et al. (1996, 1999) and Van der Veen (1998a, 1999a,b), who applied linear elastic fracture mechanics (LEFM) to model the dimensions of surface crevasses. There are a number of difficulties in applying LEFM to crevasse formation and calving (Weiss, 2004), notably that the assumption of linear-elastic rheology is not met in glacier ice (Van der Veen, 1998a; Petrenko and Whitworth, 1999). The LEFM approach, however, does offer advantages, particularly the ability to deal with the effect of stress concentrations and mixed mode failure. Van der Veen's approach determines the crevasse depth for which calculated stress intensity factors exactly balance the fracture toughness of the ice, for specified ice thickness, crevasse spacing and applied stresses. Fig. 4A shows modelled stress intensity factors vs. fracture depth for four values of the applied tensile stress. Cracks will propagate so long as the stress
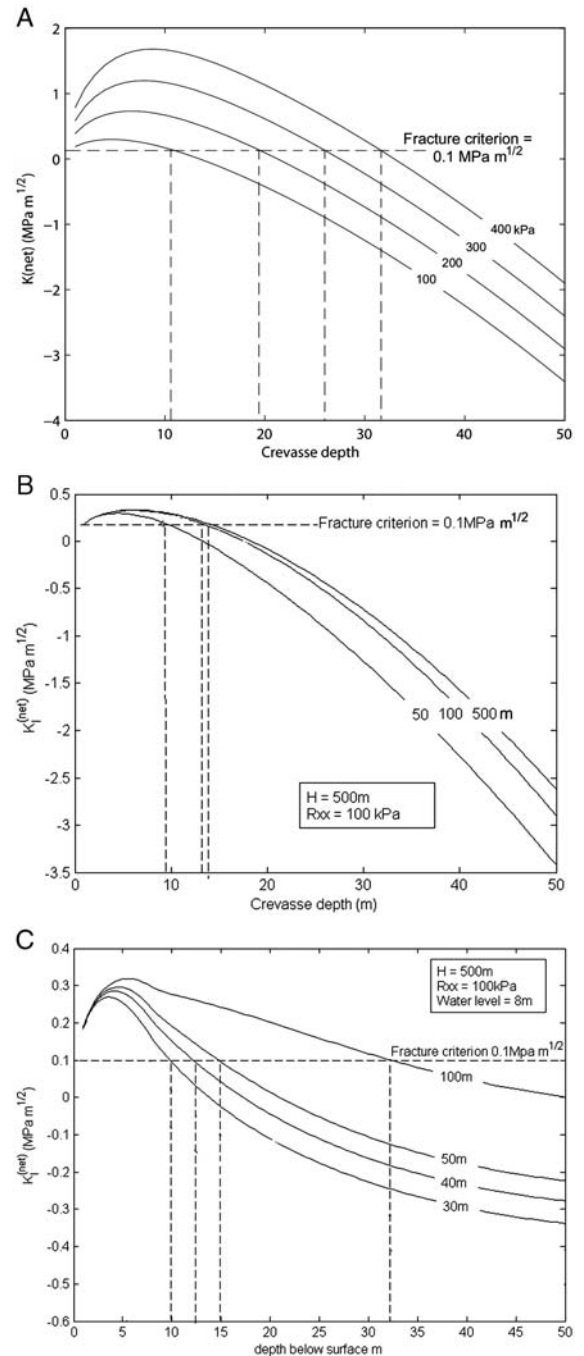

Fig. 4. (A) Stress intensity factors (K(net)) and predicted crevasse depths for a fracture criterion of 0.1 MPa m$^{0.5}$ and applied tensile stresses of 100, 200, 300 and 400 kPa, using the Van der Veen (1998a) LEFM model. (B) Effect of crevasse spacing on modelled crevasse depth in the Van der Veen (1998a) model. Crevasse depth is less for closely-spaced crevasses because stress concentration effects are reduced. (C) Modelled crevasse depths for water level 8 m below the glacier surface, for crevasse spacings of 30, 40, 50 and 100 m.

intensity factor exceeds the fracture criterion, 0.1 MPa m$^{0.5}$ in the example shown. The modelled stress intensity factors are below the failure criterion at shallow depths in the ice, and are insufficient to allow crevasse penetration through surface ice, unless pre-existing cracks of sufficient length exist. The critical crack length is 0.5 m for a tensile stress of 100 kPa, less for higher stresses. After an initial increase, stress intensity factors diminish with depth, eventually falling below the fracture criterion. This is the predicted crevasse depth. Crevasse spacing exerts a strong influence on modelled stress intensity factors and crevasse depths (Fig. 4B).

Rist et al. (1999) used an LEFM approach to model fractures on the Filchner–Ronne ice shelf. Their modelling, which assumes the presence of initial flaws of between 5 and 50 cm in length, reproduces areas of crevassing convincingly well when compared with satellite imagery. This work is particularly well founded, because it employs a fracture criterion established by laboratory testing of ice recovered from Antarctic ice cores.

Relatively few attempts have been made to compare the predictions of crevasse-depth functions with observations (e.g. Meier, 1958; Nye, 1959; Holdsworth, 1969a). An analysis of available data by Holdsworth (1969a) found a good fit between observed crevasse depths and those predicted by Eq. (10), although the model tended to over-estimate crevasse depth, possibly because zero yield stress was assumed. Recent observations in crevasse fields at Breiðamerkurjökull (Mottram and Benn, unpublished data) show that the Nye and Van der Veen models perform similarly in predicting crevasse depth from measured strain rates, suggesting that simple formulations such as Eq. (10) may be adequate for many applications. Because the Weertman method was formulated for isolated crevasses, it consistently over-estimates the depths of crevasses in fields.

The presence of water can exert a strong influence on the depth of surface crevasses (Weertman, 1973; Robin, 1974; Van der Veen, 1998a; Alley et al., 2005). By opposing cryostatic pressure, water will allow crevasse propagation to greater depths, and if sufficient water is available, a crevasse may penetrate to the bed of the glacier. The effect of water can be incorporated into the Nye (1957) crevasse depth formula as follows:

$$d = \frac{2}{\rho_{I}g}\left[\left(\frac{\dot{\varepsilon}}{A}\right)^{\frac{1}{n}} + (\rho_{W}gd_{w})\right] \tag{11}$$

where ρ_{W} and d_{w} are the density and depth of water in the crevasse, respectively. Water-filled crevasses were also considered by Van der Veen (1998a; Fig. 4C). Water can flow into crevasses following surface melt (e.g. Scambos et al., 2000) or if a free connection exists with the sea or a proglacial lake, which is most likely to be the case where the crevasse is located close to the glacier margin.

The presence of water is particularly important for the penetration of basal crevasses (Van der Veen, 1998b). Because ice overburden pressures increase rapidly with depth, very high basal water pressures and high tensile stresses are required to allow basal crevasse development, as well as pre-existing fractures of critical length. Although it is likely that basal crevasses play a role in some calving processes (e.g. Venteris, 1997) insufficient observations are currently available to allow testing of the Van der Veen model.

3.4. Crevasse orientation

In classical theory (Nye, 1952; Van der Veen, 1999a), crevasses are regarded as Mode I fractures that form normal to the direction of maximum extension, determined from the relative values of the three strain rate components. Strain rates in the map plane can be defined in terms of the surface velocity components U_{S} and V_{S}, parallel to the x (longitudinal) and y (transverse) directions, respectively:

$$\dot{\varepsilon}_{xx} = \frac{\partial U_{S}}{\partial x} \tag{12}$$

$$\dot{\varepsilon}_{yy} = \frac{\partial V_{S}}{\partial y} \tag{13}$$

$$\dot{\varepsilon}_{xy} = \frac{1}{2}\left(\frac{\partial V_{S}}{\partial x} + \frac{\partial U_{S}}{\partial y}\right) \tag{14}$$

The orientation of the principal extensional strain axis, θ, relative to the larger of $\dot{\varepsilon}_{xx}$ and $\dot{\varepsilon}_{yy}$ is:

$$\tan 2\theta = \frac{2\dot{\varepsilon}_{xy}}{(\dot{\varepsilon}_{xx} + \dot{\varepsilon}_{yy})} \tag{15}$$

When deformation consists only of pure shear (Eqs. (12) and (13)), transverse crevasses will form under longitudinal extension, and *vice versa*. Alternatively, when all deformation is by simple shear (Eq. (14)), crevasses will be oriented at 45° to the direction of shear. Intermediate orientations will occur for different combinations of pure and simple shear (Nye, 1952). Several studies have made use of this model to infer surface strain patterns, and therefore surface stresses, from crevasse orientations (e.g. Vornberger and Whillans, 1990).

Most field measurements, however, have found that crevasses are not perfectly aligned with the principal stress axes (Kehle, 1964; Whillans et al., 1993). Van der Veen (1999a,b) argued that this probably reflects mixed mode failure, and cited multiple examples from the literature of displacement patterns indicative of Mode II fracture superimposed on Mode I fracture. An additional difficulty in determining exact relationships between stress fields and crevasse patterns is the advection and rotation of crevasses following their formation.

At calving termini, the suites of crevasses that define the geometry of calved blocks frequently consist of crevasses advected passively to the terminus and new crevasses forming in response to near-terminus stress
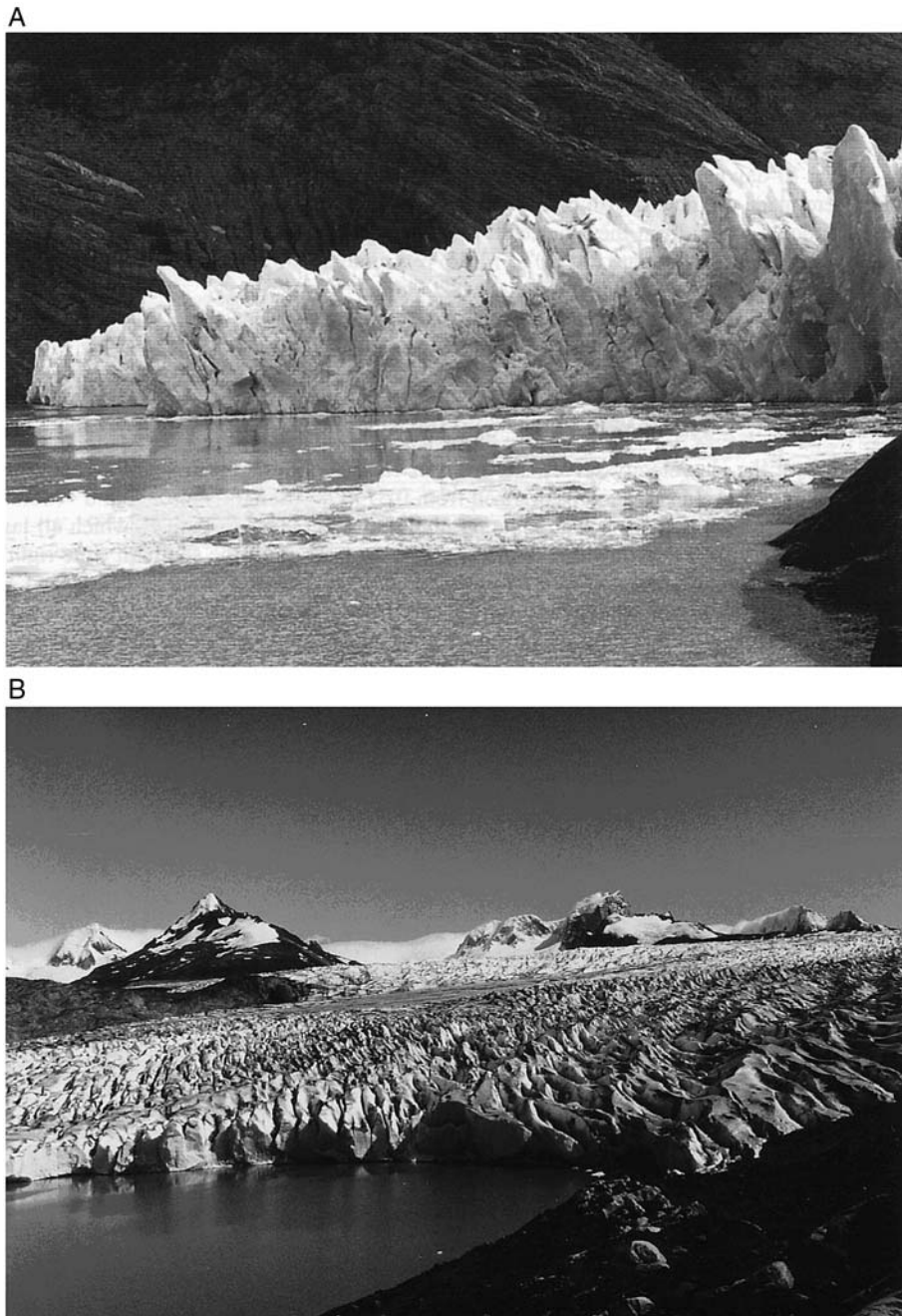

Fig. 5. Pre-existing and new fractures at calving margins, Patagonia. (A) Glaciar Ameghino, December 1993; (B) Glaciar Upsala, east terminus, March 1993.

fields (Fig. 5). We now consider the range of situations in which pre-existing and new fractures can propagate, and their role in triggering different types of calving events.

4. Calving processes

Calving is not a single process, but a family of related processes that can take place in a wide variety of settings. Calving glacier margins may be grounded or floating. This distinction, however, is not clear-cut, but encompasses a wide spectrum from essentially terrestrial glaciers terminating in shallow water, through glaciers lightly grounded in deep water or with near-buoyant or locally buoyant termini, to fully floating ice shelves. Calving

glaciers occur in a wide range of climatic environments, from arid polar to monsoonal sub-tropical mountains, and can consist of polar, polythermal or temperate ice. They may be fast or slow-flowing, or surging. The proglacial water body in which they terminate may be either tide-water or freshwater, with varying water body properties including temperature and stability. The calving family also includes dry calving at terminal cliffs in arid polar environments (Smiraglia et al., 2004). The seemingly endless variety in calving margins arises from permutations of these and other factors, although some combinations do not occur. For example, ice shelves only occur where mean annual temperature is ≤ 5 °C (Mercer, 1978; Scambos et al., 2000), although near-buoyant or locally
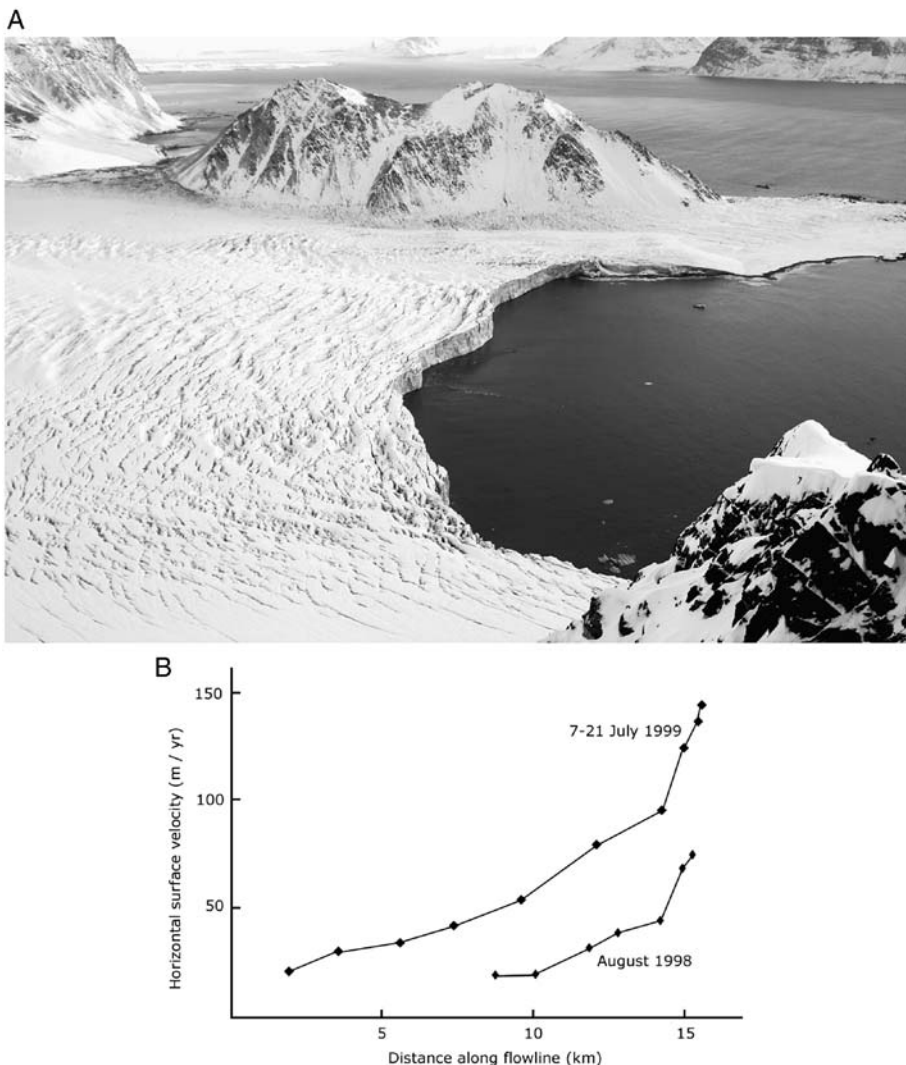

Fig. 6. (A) Hansbreen, Svalbard. (B) Velocity profiles from 1998 and 1999. The large differences in velocities between years reflects variations in basal hydrology. Adapted from Vieli et al. (2004).

buoyant termini can also occur on polythermal or temperate glaciers in warmer environments (e.g. Warren et al., 2001; Skvarca et al., 2002; Motyka et al., 2003b; O'Neel et al., 2003; Boyce et al., in press).

We can identify a range of possible situations where stresses can be high enough to allow fractures to propagate through glacier ice, and trigger calving events: (1) during stretching of ice associated with spatial gradients in the velocity of a glacier; (2) as the result of force imbalances in the vicinity of ice cliffs; (3) where ice cliffs are undercut by preferential melting at or below the waterline; and (4) where torque is introduced by buoyant forces.

Each of these situations is examined in turn below.

4.1. Stretching associated with surface velocity gradients

Tensile stresses associated with along-flow and across-flow gradients in ice velocity are commonly large enough to initiate crevasse formation on glaciers and ice shelves. On many calving glaciers, a combination of dominantly simple shear near the glacier margins and longitudinal extension nearer the centreline creates a distinctive arcuate crevasse pattern, which can be mirrored by the form of embayments in the calving front to a remarkable degree (Fig. 6). This correspondence suggests that crevasses which have opened in response to velocity gradients at the glacier scale provide an important first-order control on the position and geometry of calving margins, by providing preferential lines of weakness near the glacier terminus (Powell, 1983). The role of surface strain rates in preconditioning calving is nicely illustrated by the effects of changing strain patterns on surging glaciers (Dowdeswell, 1989), and a particularly striking example is provided by the 1993–95 surge of Bering Glacier, Alaska (Lingle et al., 1993; Post, 1997; Roush et al., 2003). Prior to the arrival of the surge front at the calving terminus, the quiescent ice surface was unfractured and calving consisted of low frequency events, whereas after the arrival of rapidly-straining ice, calving from the shattered terminus became prolific, producing myriads of small icebergs.

On glaciers with grounded calving margins, ice velocities typically increase towards the terminus, forming fields of transverse crevasses where longitudinal strain rates are sufficiently high (Fig. 6; Meier and Post, 1987; Warren and Aniya, 1999; Vieli et al., 2000; O'Neel et al., 2001). Large increases in velocity near glacier termini are attributable to accelerating basal motion consequent on diminishing effective pressure, and thus drag, at the bed as the glacier approaches flotation (Vieli et al., 2000; O'Neel et al., 2005). The fact that basal velocity and longitudinal strain rates commonly increase close to the termini of tidewater glaciers provides a plausible explanation for the

inverse relationship between calving rate and height above buoyancy (Sikonia, 1982), and the Van der Veen and Vieli height above buoyancy criteria (Section 2.3). In some cases, however, velocity gradients have been observed to diminish very close to calving fronts. For example, on Le Conte Glacier, Alaska, O'Neel et al. (2001) noted that strain rates increase to within about 200 m of the terminus, where an abrupt decrease occurs. Similar patterns have been observed on Columbia Glacier, Alaska, (Krimmel, 2001) and Breiðamerkurjökull, Iceland (Björnsson et al., 2001), and may indicate decoupling of the glacier from its bed close to the terminus. This phenomenon and its significance for calving are examined further in Section 4.4.

A relationship between velocity patterns, crevasse formation and calving events is also apparent on ice shelves. On the ice shelves fringing continental Antarctica, the largest calving events involve the release of tabular icebergs following the propagation of *rifts*, or crevasses that penetrate the full thickness of the shelf (Lazzara et al., 1999; Joughin and MacAyeal, 2005). Rifts are initiated in areas of high strain rates, such as where floating ice shears past grounded ice or land masses, or where longitudinal or lateral spreading rates are high (Fig. 7). Once rifts have formed, a variety of factors can cause them to propagate across the shelf until they intersect other rifts or the shelf edge, eventually isolating tabular bergs, sometimes of immense size. Although initial rift formation can be understood in terms of large-scale flow patterns, associated calving events are highly episodic and complex in detail, and to date have been modelled only on a case-by-case basis (e.g. Larour et al., 2004a,b; Bassis et al., 2005).

As noted in Section 3.3, crevasse propagation through the full thickness of a glacier or ice shelf is greatly facilitated by the presence of surface water. This was dramatically illustrated by the recent catastrophic break-up of ice shelves fringing the northern Antarctic Peninsula. Scambos et al. (2000) showed that break-up of the Larsen A and B, and Wilkins ice shelves was preceded by the formation of extensive melt ponds, indicating large volumes of stored meltwater, which would fill any surface crevasses. Using the Van der Veen (1998a) crevasse model, Scambos et al. (2000) argued that longitudinal strain rates on the ice shelves were not sufficiently high to promote rift formation in the absence of meltwater. When shallow surface crevasses were filled with water, however, the additional force opposing cryostatic pressure allowed them to propagate downward without limit, leading to full-depth rifting. This process appears to have occurred nearly simultaneously over large portions of the ice shelves, precipitating catastrophic break up. The force exerted by large blocks as they turn over during calving also appears to be a significant factor in the near-simultaneity of ice
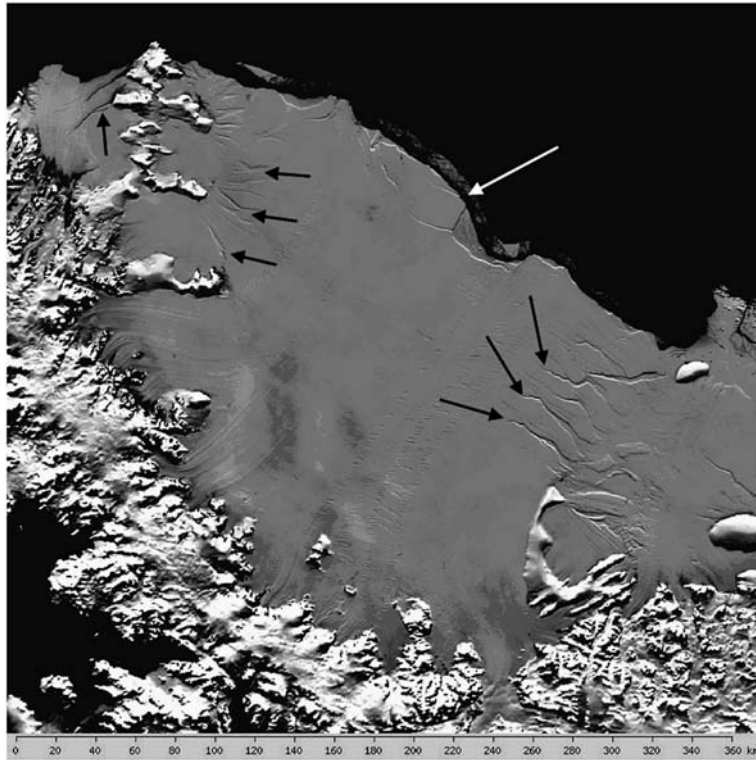
Fig. 7. MODIS image of Larsen ice shelf, Antarctic Peninsula. Prominent rifts (indicated by black arrows) occur in areas of high extending flow. Rift growth is in the process of isolating a large tabular berg (white arrow). Image from http://nsidc.org (Haran et al., 2005).

shelf collapse (MacAyeal et al., 2003). The presence or absence of surface meltwater thus appears to be a crucial factor in determining the location and style of calving on these ice shelves.

4.2. Force imbalance at terminal ice cliffs

In one of the earliest models of calving processes, Reeh (1968) showed than a force imbalance exists near the terminus of a floating glacier terminus or ice shelf. Above the waterline, the cryostatic pressure at the terminal face is essentially unopposed by atmospheric pressure, while below the waterline it is always greater than the pressure exerted by the water column, except at the base (Fig. 8). The total horizontal force at the ice cliff is given by:

$$\overline{P}_I H - \overline{P}_W D_W = \frac{1}{2}\rho_I g h H \tag{16}$$

where $\overline{P}_I$ and $\overline{P}_W$ are the vertically averaged ice and water pressures, respectively, H is the ice thickness, D_W is the water depth, and h is the elevation of the ice shelf surface (Paterson, 1994). This outward-acting force is unevenly distributed, and is at a maximum at the waterline. An eccentrically-applied stress results in a bending moment or torque, tending to rotate the ice front forward and down-

ward. In turn, this creates a zone of tensile and shear stresses at the ice surface, with a maximum at a distance from the front roughly equal to the ice thickness. Reeh argued that surface fractures will tend to develop in this region, promoting calving. A time-dependent finite-element model of Reeh's bending mechanism, including a representation of crack growth, was developed by Fastook and Schmidt (1982). Patterns of vertical motion near rift margins on the Ronne Ice Shelf observed by Larour et al. (2004b) provide striking evidence for flexure associated with force imbalance. The associated calving events appear to be of low magnitude and high frequency, in contrast with the calving of large tabular bergs driven by rift propagation.
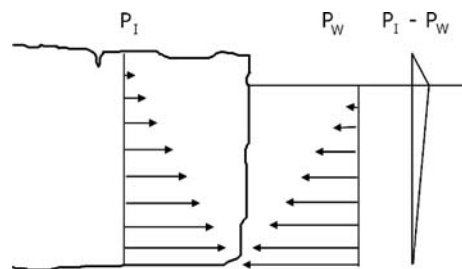

Fig. 8. Schematic cryostatic and hydrostatic forces at the terminal cliff of a floating ice shelf.

Local force imbalance clearly also influences calving processes at grounded termini, although disagreement exists over important details. Stress and strain patterns in the vicinity of subaerial ice cliffs have been analysed by Hughes (1989, 1992, 2002), Hughes and Nakagawa (1989) and Kenneally and Hughes (2002), using an ice-margin geometry based on observations at Deception Island, Antarctica. The model geometry consists of a concave, overhanging ice cliff behind which is a series of parallel, curving shear bands, identical in form to theoretical slip lines in a perfectly plastic slab under uniform extension (Nye, 1951; Hooke, 2005). According to Hughes' analysis, deformation of the ice occurs along the shear bands, in a manner likened to slippage between the pages of a book bent around its binding, leading to calving by the detachment of successive lamellae. The general applicability of this forward bending theory, however, has been questioned on several grounds, including (1) bending shear proceeds too slowly to account for calving in many settings, (2) it does not apply to glaciers that approach flotation, and (3) it is not supported by empirical observation (Meier, 1994; Van der Veen, 1996; Meier, 1997; Hanson and Hooke, 2000). Shear bands of the type described by Hughes have not been reported from any other localities. Indeed, observations of evolving ice margin geometry at different localities are inconsistent with the bending shear concept (e.g. Kirkbride and Warren, 1997; Benn et al., 2001).

Hanson and Hooke (2000, 2003) took an alternative, finite-element modelling approach to analysing the stress and velocity distribution in the subaerial and subaqueous portions of a glacier terminus. The results show a persistent maximum in tensile stress and ice velocity close to the waterline (or ice-cliff base in the case of a terrestrial margin) and a consequent tendency for the face to bulge outward at this locality. This pattern is in sharp contrast with the oversteepening of the cliff top predicted by the Hughes model. The Hanson and Hooke model also predicts oversteepening of the face below the waterline, an effect that increases with water depth. They suggested that this may provide a plausible physical explanation of the water depth/calving rate correlation, although Van der Veen (2002) has pointed out that the modelled rate of overhang development is much lower than most observed calving rates. Hanson and Hooke (2003) also suggested that the modelled pattern of tensile stresses near the waterline may explain why observed calving cliff heights rarely exceed 70 m because higher ice faces will be subject to very high stresses and rapid failure.

4.3. Undercutting by subaqueous melting

Where melt rates at or below the waterline exceed subaerial melt rates, terminal ice cliffs will be progressively undercut, increasing force imbalances at the margin and encouraging calving failure. Undercutting may occur in two ways, by enhanced melting (1) at the waterline, leaving the subaerial portion of the terminus overhanging a subhorizontal waterline notch, or (2) below the waterline, resulting in the subaerial cliff projecting above an undercut subaqueous cliff.

Iken (1977) developed a finite-element model of the evolution of an ice block undercut by a waterline notch. A shallow crack was prescribed at the glacier surface behind the terminus, where tensile stress was at a maximum, and the model simulated the subsequent interaction between the stress field, the growing crack, and the evolving block geometry. As the crack propagates downward, the detaching ice block tips outward, creating an increasingly overhanging front face. This increases the tensile stress at the crack tip, promoting further crevasse growth until failure occurs. This sequence of events, and the geometry of the resulting failure surface, is remarkably similar to some examples of block calving observed at the margins of shallow supraglacial ponds (Benn et al., 2001). Many other types of failure occur in the vicinity of waterline notches, however. Notch roofs are particularly prone to collapse along long, arch-shaped fractures. The location and timing of calving above waterline notches, as well as the precise geometry of the failure surface, is strongly influenced by the presence of pre-existing lines of weakness such as crevasses or debris bands. Fig. 9 shows a pair of photographs of part of the margin of Breiðamerkurjökull, in which individual calving events are clearly controlled by pre-existing crevasse traces. In other situations, new fractures develop as a result of evolving stress conditions, which then define the location and size of calving events (Fig. 10).

Studies at freshwater ice margins in New Zealand (Kirkbride and Warren, 1997, 1999; Purdie and Fitzharris, 1999; Warren and Kirkbride, 2003), the Himalaya (Benn et al., 2001) and Patagonia (Warren, 1999; Haresign and Warren, 2005) have documented cyclic calving behavior involving waterline melting and upwards growth of an overhang by spalling of progressively larger lamellae (Fig. 10). The cycle sometimes concludes with subaqueous calving from a projecting 'ice foot' or submerged platform (Section 4.4). A very similar pattern has been reported from the tidewater Hansbreen in Svalbard by Vieli et al. (2002), showing that this calving mechanism is not unique to freshwater sites as once suspected. In such situations, calving decreases to near zero in winter, especially when lake or sea ice forms (Vieli et al., 2002). This is presumably the reason why, for lake-calving glaciers, a positive correlation exists between U_C and water
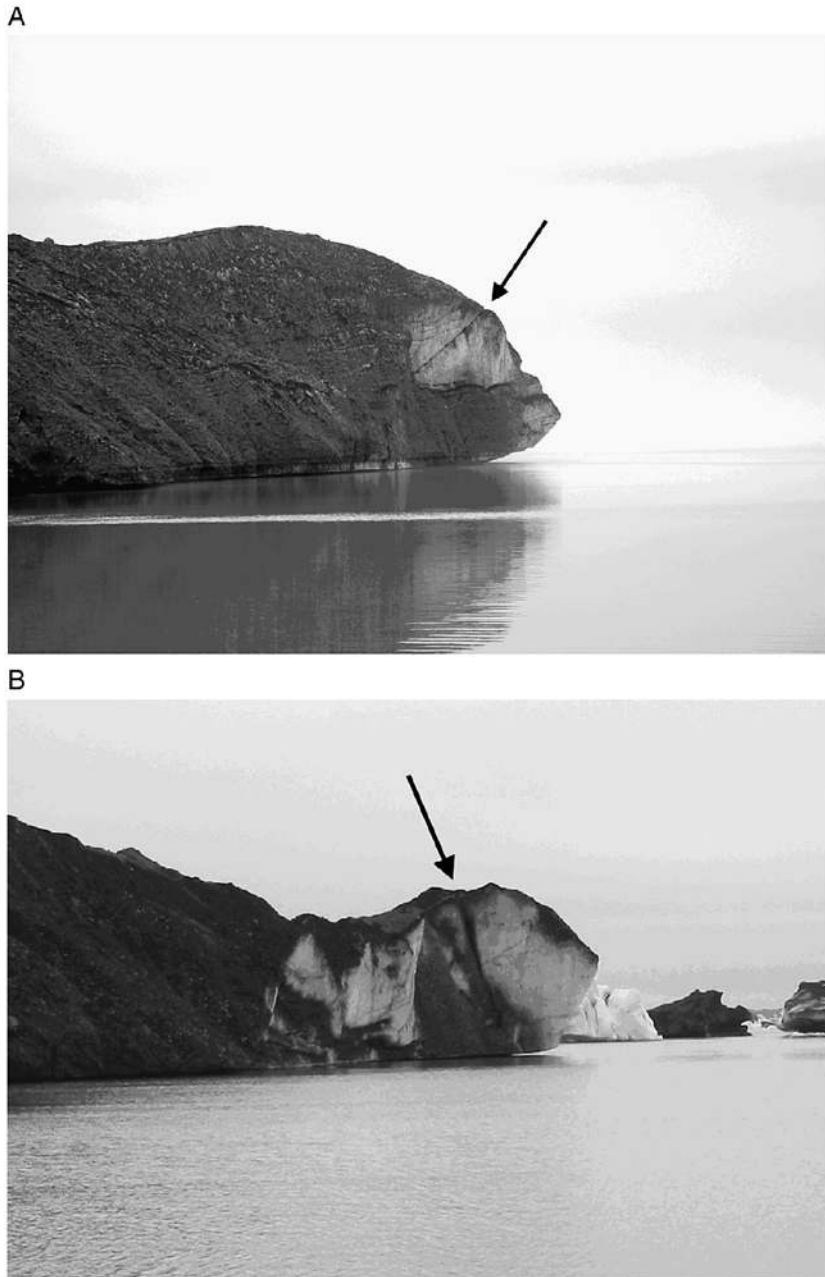
Fig. 9. Episodic waterline melt-driven calving, Breiðamerkurjökull, Iceland. (A) August 7 2004. (B) July 24 2005. The terminal overhang follows the line of the crevasse trace arrowed in panel A. A second calving event occurred 2 days later along the crevasse trace arrowed in panel B.

temperature, a correlation which is as strong as that between U_C and water depth (Warren and Kirkbride, 2003).

Detailed measurements of melt rates in waterline notches have been made by Röhl (2006) at the terminus of Tasman Glacier, New Zealand. Notch formation rates typically vary between 10 and 30 cm d^{-1} in summer, corresponding to a mean calving rate of 34 m yr^{-1}. Notch

deepening is most efficient where water levels are relatively constant, as energy transfer from warm surface water is focused in a narrower band of ice. No significant relationship was found between water temperature and melt rate, possibly due to the complicating influence of water circulation (cf. Eijpen et al., 2003). Because melt rate depends not only on the temperature field in the proglacial water body, but also the rate at which cooled water is

Fig. 10. Vertical fractures and detaching lamellae at the margin of lake-calving glaciers, New Zealand. (A) Maud Glacier, March 1995. Note the waterline notch and overhanging ice cliff. (B) Godley Glacier, April 1994. The ice lamella measures c. 18 m high × 14 m wide × 1 m thick.

evacuated from the ice face and replaced by relatively warm water, calculating subaqueous melt rates is beset by uncertainty (e.g. Motyka et al., 2003a). Theoretical and laboratory studies (e.g. Russell-Head, 1980; Josberger and Martin, 1981; Eijpen et al., 2003) have focused on water circulation driven by thermal variations in the water column (free convection), and conclude that melt rates are generally small, comparable with the low end of observed values of U_C. However, forced convection driven by vigorous meltwater upwelling is typical at many calving fronts, especially in temperate tidewater settings, and could result in much higher energy fluxes and melt rates than is possible by free convection. Warren et al. (1995b) presented evidence indicating significant rates of subaqueous melting at Glaciar San Rafael, Chile. Hanson and Hooke (2000) pointed out that there may be sufficient energy in far-field water to melt ice at rates in the range of observed calving speeds if this energy can be advected to the ice face by convection processes associated with upwelling and/or tidal action. Recent evidence supports this suggestion, indicating that subaqueous melt rates may be considerably higher than previously thought, even reaching rates com-

parable with total calving losses (Haresign and Warren, 2005). Motyka et al. (2003a) concluded that subaqueous melting may account for at least as much ice loss as calving at the terminus of tidewater LeConte Glacier, Alaska, and that melting may trigger rapid calving by strongly undercutting the subaerial cliff. Conversely, where ice proximal water temperatures are close to 0 °C, calving rates may be very low (Kennett et al., 1997). It seems increasingly clear that the nature of the ice-contact water body, and in particular its thermal regime and the characteristics of the circulation pattern, has a crucial influence on calving through its influence on the geometry and hence the stress distribution within the terminus.

4.4. Torque arising from buoyant forces

Buoyant forces may trigger fracture propagation and calving failure in two main situations. First, calving losses above the waterline may exceed those below, causing the development of a projecting subaqueous 'ice foot', which may fail catastrophically. Second, surface melting can cause the terminal zones of hitherto grounded glaciers to

become buoyant, leading to calving when buoyant forces become sufficiently high.

The dangers of subaqueous calving events were well known to Inuit kayakers, as recorded by Fridtjof Nansen in '*The First Crossing of Greenland*': "far away from [the glacier], out at sea, huge masses of ice may suddenly dart up from the depths and annihilate both boat and crew. The name Puisortok…means 'the place where something shoots up'" (Nansen, 1890). Subaqueous calving events are generally less frequent but larger in magnitude than subaerial calving (Warren et al., 1995b; Motyka, 1997; O'Neel et al., in press). Detailed observations of subaqueous calving have been made by Motyka (1997) at the deep water margin of Le Conte Glacier, Alaska, where events were commonly preceded by the collapse of subaerial seracs or portions of ice cliff, whereupon large tabular or oblong blocks apparently detached below the surface and rose violently parallel to the ice front. Some blocks emerged as much as 200 to 300 m from the subaerial calving front, and isolated 'shooters' up to 500 m from the ice front have been reported. Closely similar subaqueous calving behavior has been observed at Glaciar San Rafael, Chile (Warren et al., 1995b), indicative of the existence of projecting 'ice feet' (Hunter and Powell, 1998). O'Neel et al. (in press) have suggested that the close association between subaerial and subaqueous calving events reflects the sudden reduction of ice overburden pressure on the submerged portion, and the consequent increase in buoyant forces. The fact that some subaqueous calving events occur at a great distance from the ice margin, and their highly episodic nature, suggest that the presence (or absence) of pre-existing weaknesses must play an important role in the location and timing of failure. This point is supported by modeling by Van der Veen (1998b), who showed that the growth of basal crevasses is contingent on the presence of pre-existing fractures of critical length.

The terminal zones of otherwise grounded glaciers may become buoyant if surface melting thins the ice below the flotation thickness (e.g. Lingle et al., 1993; Warren et al., 2001; Benn and Warren, 2002; Boyce et al., in press). For equilibrium, the surface and basal gradients of a buoyant ice front must maintain a constant ratio, such that:

$$h = H\left(1 - \frac{\rho_{\mathrm{I}}}{\rho'_{\mathrm{W}}}\right) \qquad (17)$$

If this condition is not met, the buoyant part of the terminus must rotate to restore equilibrium, either slowly by ice creep or rapidly by fracture propagation and calving failure (Howarth and Price, 1969; Holdsworth, 1973;

Warren et al., 2001). Evidence for this process is shown in Fig. 11, which shows raised and tilted waterline melt notches in part of the terminus of Breiðamerkurjökull, Iceland. The notches mark the former position of the ice relative to the waterline, and demonstrate that part of the terminus was raised and back-tilted. Detachment of back-tilted portions of the terminus typically occurs along pre-existing crevasses some distance back from the margin, producing tabular bergs that float away without over-turning. In this context, it is interesting to note the reduction in longitudinal strain rates near the terminus of Breiða-merkurjökull observed by Björnsson et al. (2001), which suggests that, as the glacier approaches flotation basal drag vanishes and the glacier decouples from its bed. As surface melting proceeds, the glacier terminus becomes increas-ingly out of buoyant equilibrium, producing large bending forces near the junction with non-buoyant ice. Pre-existing crevasses in this region will determine the precise location of failure through stress-concentration effects, playing a similar role to the notches in the top of a chocolate bar. On some glaciers, the buoyant-torque mechanism appears to be responsible for the detachment of large portions of the terminus, producing tabular bergs hundreds of metres across (e.g. Lingle et al., 1993; Warren et al., 2001). Im-portant new observations of buoyant uplift and calving have been made at the terminus of Mendenhall Glacier, Alaska, by Boyce et al. (in press). They show that, when the glacier is approaching instability, individual calving events can be triggered by rapid surface ablation or rises in lake level. The buoyant calving process is highly episodic, but in the long term must be paced by the retreat of the grounding line as determined by surface and basal melt rates.

Oscillation of floating ice shelves can also produce bending forces large enough to trigger rift formation and calving. Periodic flexing can be directly forced by tides and ocean swells (Holdsworth, 1969b; Lingle et al., 1981; Reeh et al., 2003; MacAyeal et al., 2006), or induced by resonant filtering of ocean wave energy whereby the shelf selects its own oscillation frequency from a broad range of input wavelengths (Holdsworth and Glynn, 1981; Jeffries, 1985). The energy for individual calving or berg break-up events can therefore be provided from a variety of oceanic and atmospheric sources, including some transmitted over great distances. MacAyeal et al. (2006) showed that the break-up of a large tabular berg calved from the Ross Ice Shelf occurred immediately after the arrival of a sea swell gene-rated by a storm in the Gulf of Alaska six days previously.

4.5. A hierarchy of calving mechanisms

From the foregoing, it can be seen that varying factors can control the frequency and magnitude of calving

processes, depending on the relative importance of the four mechanisms discussed above. Considering each individually, the likely controls on calving pro-

cesses are as follows (for simplicity, we ignore fracture growth in the y (transverse) direction, and focus on the 2-D case).

Fig. 11. (A) Back-tilted block at the terminus of Breiðamerkurjökull, September 9, 2004. (B) Tilted waterline notch on buoyant, partially detached tabular berg, Breiðamerkurjökull, August 5, 2005. (C) Water-filled rift at the point of detachment of the tabular berg shown in (B). (D) Buoyant terminal zone of Glaciar Nef, Patagonia, February 1998.
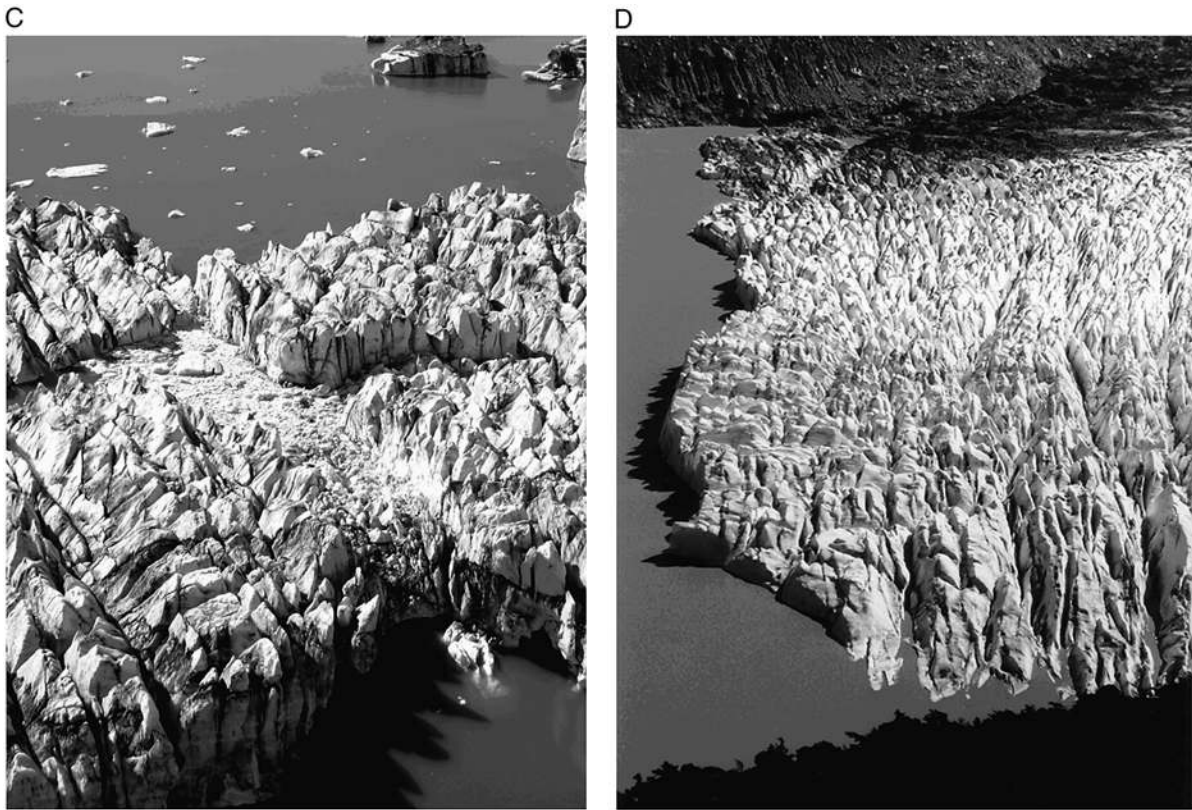
Fig. 11 (*continued*).

4.5.1. Mechanism (1): Stretching in response to large-scale velocity gradients

If surface velocity gradients constitute the only factor controlling fracture propagation, calving will occur where velocity gradients are sufficiently high to allow crevasses to penetrate through the glacier. Given that water-filled crevasses can propagate downward without limit (Section 3.3), the calving margin will be located approximately at the point where surface crevasses reach sea or lake level (assuming there is a free connection between crevasse and the sea or lake. The margin position will therefore be determined by the velocity distribution at the glacier surface (which controls crevasse depth) and the ice height above the waterline (which determines whether a crevasse of a given depth will reach the waterline). Meltwater stored in surface crevasses will cause them to penetrate deeper than dry crevasses, providing an additional, transient control on the position of the calving margin. Examples of meltwater-driven calving include the catastrophic break-up of the Larsen ice shelves following met-pond formation (Scambos et al., 2000) and accelerated calving during and after heavy rain (Kirkbride and Warren, 1997; O'Neel et al., 2003).

In the longitudinal stretching mechanism, calving is controlled by those factors that determine the ice thickness (e.g. surface mass balance and ice flux) and velocity (e.g. the driving and resisting stresses). This mechanism is compatible with the view of calving as 'slave', as an essentially passive process responding to changes in ice thickness and/or glacier dynamics. However, it does not preclude the possibility that feedback processes on longer timescales may allow calving to be a 'master', by initiating changes near the margin which may then propagate upglacier (*cf*. Meier and Post, 1987).

4.5.2. Mechanism (2): Force imbalances at unsupported ice cliffs

Where fractures are generated and propagated entirely in response to unbalanced stresses at subaerial and/or sub-aqueous ice cliffs, calving is controlled by glacier margin geometry and ice rheology. As envisaged by Reeh (1968) and Hughes (e.g. 1998, 2002) it is a cyclic process, in which unbalanced stresses drive geometric changes in the ice margin culminating in calving failure, which in turn reinstates a condition of unbalanced stresses at the new marginal cliff. In this case, the frequency of calving events will be determined by fracture propagation rates, the rate at

which glacier terminus geometry evolves, and feedbacks between geometric changes and the fracturing process. Changes in the position of the ice margin will be determined by the magnitude of individual calving events and the length of the calving cycle, which drive ice cliff retreat, and the ice velocity, which carries the ice cliff forward.

4.5.3. Mechanism (3): Undercutting by subaqueous melting

When calving is driven by melting at or below the waterline, the long-term calving rate will equal the rate at which the subaerial part of the cliff is undermined by subaqueous melting. Calving rate will therefore be a function of water body properties such as temperature, density structure and circulation patterns. As shown by Röhl (2006), the rate of overhang development is not a simple function of total ice melt, but also depends on how that melt is focused at particular levels. A given melt amount distributed over a broad elevational range will be less effective in undercutting the ice margin than the same amount focused over a narrow range. The distribution of melt will depend on water-level fluctuations, water stratification, circulation patterns and other factors. Long-term changes in terminus position will therefore be driven by the maximum subaqueous melt rate and ice velocity, analogous to the situation in Mechanism (2).

4.5.4. Mechanism (4): Torque arising from buoyant forces

In the case of subaqueous calving events, long-term calving rates will be tied to the rate of ice foot development, in turn paced by waterline melting or retreat of a subaerial calving face. The controls on calving rate and changes in terminus position are thus similar to Mechanisms (2) and (3). Where calving occurs by the detachment of the buoyant terminal zone of otherwise grounded glaciers, long-term calving rates will be controlled by the rate of retreat of the grounding line, as determined by changes in ice thickness relative to water depth. Ice thinning can occur by surface and basal melting or by longitudinal or transverse extension (dynamic thinning), so this type of buoyant calving will be influenced by both climatic and dynamic factors.

This multi-dimensional blend of causative variables, which are frequently all on display at the same calving front, is probably a major reason why repeated attempts to derive general 'calving laws' have foundered. To make sense of this complexity, it is useful to identify a hierarchy of calving processes, each subject to various extrinsic and intrinsic controls.

Longitudinal stretching associated with the large-scale velocity structure of the glacier, can be regarded as the first-order control on calving. This is because velocity gradients determine the depth of surface crevasses, and consequently whether crevasses reach the waterline as the glacier approaches flotation. Where velocity gradients are high near the grounding line, crevasses are likely to reach water level and trigger calving, and the glacier will terminate at a grounded ice cliff. Conversely, if velocity gradients and crevasse depths near the grounding line are small, then ice can become buoyant and form a floating ice tongue or ice shelf. In conjunction with ice thickness relative to water depth, velocity gradients determine the maximum possible extent of a calving glacier (L_{MAX}), and how L_{MAX} changes through time.

Stress imbalances at the ice front, *undercutting by melting*, and the *detachment of buoyant termini* are second order processes, superimposed on the first order mechanism. This is not to say that such processes are less important, simply that they operate within the limits imposed by large-scale glacier dynamics. Although longitudinal strain rates determine the maximum possible position a glacier can attain, second-order processes can further erode the ice margin so that the glacier has a more limited extent ($L < L_{MAX}$). Indeed, where longitudinal strain rates are small, second-order processes may be the rate-controlling mechanisms on calving losses. This is particularly likely to be the case where proglacial water bodies are shallow and relatively warm, or where there are small longitudinal velocity gradients near the glacier front. We regard *buoyant calving of a submerged 'ice foot'* as a third-order process, because it is paced by first- and second-order processes.

The proposed primary role of longitudinal stretching in calving processes does not imply that there should be a straightforward correlation between longitudinal strain rates and calving rates. Indeed, observed correlations between longitudinal strain and calving rates are inconsistent in the short term and very weak on annual or longer timescales (Meier, 1994; Van der Veen, 1996). The lack of such a relationship reflects the fact that longitudinal velocity gradients are independent of absolute values of velocity. This means that particular strain rates may be associated with a very wide range of velocities, and hence rates of ice delivery to the calving front (Eq. (1)). Thus, longitudinal strain rates may act as a fundamental control on where and when calving occurs, but do not directly control calving rates.

4.6. A crevasse-depth calving criterion

The foregoing analysis suggests that first-order calving processes can be parameterised using longitudinal strain rates, ice thickness and water depth. Benn et al. (in press) proposed that the position of a calving margin
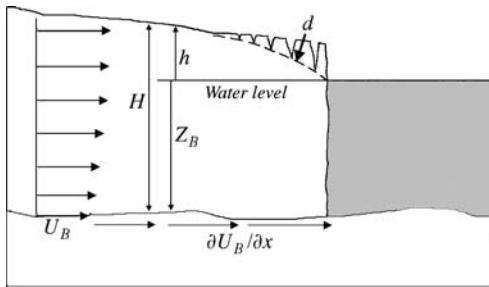
Fig. 12. Schematic illustration of first-order calving in response to longitudinal stretching. Surface crevasses propagate downward to a depth d in response to the velocity gradient $\partial U_B/\partial x$. Calving is assumed to occur when $d=h$ (after Benn et al., in press).

can be defined as the point where the depth of surface crevasses d equals the glacier 'freeboard' above sea level, h (Fig. 12):

$$x = L \text{ where } d(x) = h(x) \qquad (18)$$

where x is the horizontal co-ordinate parallel to glacier flow, positive downstream. For time-evolving ice sheet models, crevasse depths are most conveniently calculated following the Nye (1957) formulation (Eqs. (10) and (11)), because (1) crevasse depths calculated using the Van der Veen (1998a) model are sensitively dependent on crevasse spacing, which is not known *a priori*; (2) it is computationally cheap and easily incorporated into numerical schemes, and (3) it performs almost as well as more complex functions in predicting observed crevasse depths (Mottram and Benn, in preparation). In some circumstances, however, the Van der Veen (1998a) LEFM model might be preferable for calculating crevasse depths.

The crevasse-depth calving criterion is based on the idea that the downglacier velocity gradient, $\partial U/\partial x$, and the ice elevation above the waterline, h, are the primary controls on glacier terminus position. Of course, in nature other factors may influence crevasse propagation and the position of the calving margin. First, if water does not enter surface crevasses they may penetrate to, or even below, lake or sea level without propagating through the full thickness of the ice or triggering calving. This will be the case if no connections exist between surface crevasses and the proglacial water body, and surface melting is negligible. In this case, calving could be 'switched on' if surface melting increased, as appears to have occurred prior to the collapse of the Larsen ice shelves (Scambos et al., 2000). Second, as formulated here, the crevasse-depth calving criterion does not consider crevasse extent in the transverse (y) direction. For calving to occur, crevasses must completely isolate

blocks of ice, not simply penetrate from the surface to the base. This is clearly illustrated by ice shelf-rifting, where full-depth crevasses may persist for several years before they extend far enough across the shelf to release tabular bergs. Third, the crevasse-depth criterion may overestimate glacier length if other, second-order processes play a significant role in calving. For example, subaqueous melting may induce fracture propagation and calving well before the crevasse depth failure criterion is met.

With these provisos, however, the crevasse-depth calving criterion provides a simple means of parameterising first-order calving processes in ice sheet models. It is more versatile than the Van der Veen/Vieli height-above-buoyancy model, because it allows ice shelves to form. Where longitudinal velocity gradients are large, crevasses are likely to reach the waterline and penetrate the full thickness of the glacier while the ice is still grounded. On the other hand, where longitudinal tensile stresses in the vicinity of the grounding line are small, the glacier terminus will be able to float without calving occurring. Whether ice shelves are allowed to form, therefore, depends on the velocity gradients near the grounding line, which in turn depends on the factors controlling glacier velocity.

5. Ice velocity: The link between first-order calving and glacier dynamics

Glacier velocity exerts a fundamental control on calving rates in two ways. First, ice speeds at the terminus (U_T) are usually much larger than the rate in change of terminus position (dL/dt), so that a good correlation between calving rates and glacier speed should be expected from Eq. (1), except during times of rapid terminus retreat (Van der Veen, 1996). Second, longitudinal and transverse velocity gradients determine both the depth of surface crevasses and rates of dynamic thickness change, and are therefore primary controls on calving processes (Sections 4.1 and 4.5). The behavior of calving glaciers, therefore, depends critically on glacier velocity and its variations in space and time. Basal motion is a prerequisite for fast flow and high longitudinal strain rates. In this section, we examine the controls on basal motion, and the implications for calving and related dynamic processes.

5.1. Force balance

Glacier velocity and its derivatives depend on the magnitude of the driving stress, the mixture of forces resisting flow, and their variations in space and time. Van

der Veen and Whillans (1987) defined the large-scale force balance of a glacier as:

$$\tau_D = \tau_B - \frac{\partial}{\partial y}(H\overline{R}_{xy}) - \frac{\partial}{\partial x}(H\overline{R}_{xx}) \quad (19)$$

where τ_D is the driving stress. The first term on the right-hand side is basal drag, the second term is resistance to flow arising from lateral drag, and the third term is resistance arising from longitudinal stress gradients. $\overline{R}_{xy}$ and $\overline{R}_{xx}$ denote the vertically averaged lateral shear stress and longitudinal deviatoric stress, respectively. The driving stress is given by:

$$\tau_D = \rho_I g H \frac{\partial h}{\partial x} \quad (20)$$

Temporal velocity fluctuations on short time scales largely reflect variations in resisting stresses, because significant changes in driving stress require large adjustments to glacier geometry. Longer term changes in velocity can reflect either changes in resistance or driving stress (e.g. Iken and Truffer, 1997). It is useful to consider the role of basal drag, lateral drag, and longitudinal stress gradients individually, before examining the ways in which they act in combination to control speed and strain rates on calving glaciers and ice shelves.

5.2. Basal drag

Drag at the bed of a glacier is a complex function of ice temperature, the pressure, volume and distribution of subglacial water, debris content, and other factors. Where the basal ice is below the pressure melting point, the ice-bed interface has high strength and little or no basal motion is possible. Where water is present, significant basal motion can occur by a variety of processes, including sliding (involving regelation, enhanced creep around obstacles and cavitation at the ice-bed interface), deformation of subglacial sediment, and ploughing of the ice sole over soft sediments (e.g. Lliboutry, 1968; Boulton and Hindmarsh, 1987; Iverson et al., 1995; Tulaczyk et al., 2000; Kavanaugh and Clarke, 2006). Increasing water pressure reduces drag by reducing ice-bed coupling and solid-to-solid contact forces (Iken, 1981; Iken and Bindschadler, 1986; Schweizer and Iken, 1992; Cohen et al., 2005). Basal drag vanishes when ice is fully supported by water pressure.

Physically-based models relating basal motion to driving stress and basal drag (e.g. Fowler, 1987; Schweizer and Iken, 1992; Cohen et al., 2005) are difficult to apply at the glacier scale due to the need for detailed knowledge about the subglacial hydrological system and the form of

the bed. Consequently, simple empirically-based velocity functions are commonly used in glacier and ice sheet models, in which the effect of basal drag is parameterized using the effective pressure, P_E:

$$P_E = \rho_I g H - P_W \quad (21)$$

where P_W is basal water pressure. Determining appropriate values of P_E presents a major challenge, because of the complex relationship between discharge, volume of stored water, and the basal water pressure averaged across the bed (*cf.* Iken and Truffer, 1997). The most widely-used pressure-dependent sliding law is that introduced by Budd et al. (1979):

$$U_B = k\tau_B^P P_E^{-Q} \quad (22)$$

where k, P and Q are empirically determined scaling factors. Generalizing Eq. (22) to include cold-based glaciers, Budd and Jenssen (1987) added a temperature-dependent exponential term:

$$U_B = k\tau_S^P P_E^{-Q} \exp[\upsilon(T^* - T_O)] \quad (22a)$$

where υ is a temperature correction factor $(0.1\ \mathrm{K}^{-1})$, T^* is the basal ice temperature and $T_O = 273$ K. In practice, the values of k, P and Q are highly variable, both between and within glaciers (Bindschadler, 1983; Raymond and Harrison, 1987). Iken and Truffer (1997), for example, found that the coefficient k varied for different parts of the advance–retreat cycle of a single glacier, apparently as the result of structural reorganization of the basal hydraulic system. Using the Columbia Glacier dataset (Krimmel, 2001), Nick (2006) obtained the values $k = 9.2 \times 10^6$ m yr^{-1} Pa$^{0.5}$, $P = 3$ and $Q = 3.5$.

Several authors have suggested that the recent acceleration of calving outlet glaciers in Greenland reflects reduction of basal effective pressure as a result of increased inputs of meltwater from the surface to the bed (e.g. Krabill et al., 1999; Thomas et al., 2000). Recently, this idea has gained in currency following observations of concomitant increases in surface melt and flow speed in the interior of Greenland (Zwally et al., 2002). Numerous studies, however, have established that for outlet glaciers the relationships between meltwater flux, basal water pressure and sliding speed are not straightforward. Although increases in sliding speed are often observed at times of increasing meltwater production, the effect is typically transient. For example, on Columbia Glacier, Meier et al. (1994) and Kamb et al. (1994) observed speedup events lasting around 3 days beginning at times of increased input of water from rain or enhanced surface melting. Some of

these were followed by extra-slowdown events in which sliding speeds fell below their pre-speedup values. The extra-slowdowns were interpreted as the result of reorganizations of the subglacial drainage system, allowing higher discharges to be accommodated more efficiently. Transient speedup events have also been observed on other tidewater glaciers, including LeConte Glacier, Alaska (O'Neel et al., 2001) and Hansbreen, Svalbard (Vieli et al., 2004). At both sites, increases in velocity were attributed to increased water *storage*, rather than meltwater production or discharge. Reorganisations of the basal drainage system are also believed to underlie observed seasonal velocity variations of Columbia Glacier, with a maximum in early spring (when water storage is increasing) and a minimum in early fall (when discharges are high, but storage is relatively low; Krimmel and Vaughn, 1987; Krimmel, 1987). The ability of subglacial hydrological systems to adjust in order to accommodate higher discharges led Vieli et al. (2004) to conclude that 'a general increase in meltwater supply as a consequence of a warming climate is not expected to enhance mean basal motion'. A similar conclusion was reached by Pritchard and Vaughan (in press), who found no correlation between calculated surface melt rates and temporal trends in glacier velocities on the Antarctic Peninsula.

In models of calving glaciers, it is commonly assumed that a minimum subglacial water pressure is set by the elevation of the bed relative to the proglacial water body (Meier and Post, 1987; Van der Veen, 1999b; Vieli et al., 2000, 2001). For purely hydrostatic conditions, this assumption breaks down because the pressure head associated with the standing water will
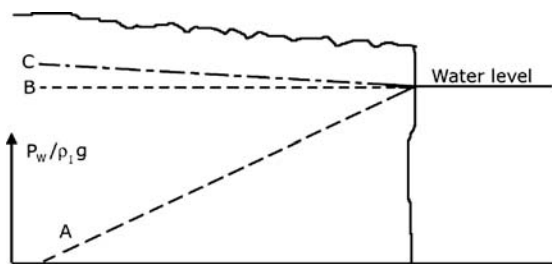

Fig. 13. Idealised basal water pressure distributions in a subglacial aquifer. (A) Under purely hydrostatic conditions, the pressure head associated with the proglacial water body decays upglacier, because of the hydraulic conductivity of the aquifer. (B) Before water can be discharged through the aquifer, pressure must everywhere exceed the minimum value set by proglacial water level. (C) For water to be discharged, pressure must rise upglacier with a gradient dependent on the discharge and hydraulic conductivity. Water pressures are expressed as the equivalent piezometric surface ($H_P = P_W / \rho_I g$), although it is not implied that such a surface exists within the glacier.

decay with distance, at a rate depending on the hydraulic conductivity of the bed (Fig. 13). Where basal water is evacuated towards the glacier margin, however, the same resistance that causes progressive hydrostatic head loss upglacier must be overcome to allow meltwater to flow downglacier. The two effects therefore exactly cancel, so that the minimum water pressure condition applies at all distances from the margin. This condition is independent of the hydraulic conductivity of the bed, although it does depend on the *connectivity* of the basal hydraulic system. Connectivity is likely to be high for fast flowing glaciers, where subglacial melting rates are large, and meltwater must be evacuated from all parts of the bed towards the margin.

In view of the above, water pressure beneath a water-terminating glacier can usefully be defined in terms of a bed elevation component and an additional component associated with the storage and flux of meltwater:

$$P_W = \rho_W g Z_B + \phi \qquad (Z_B \leq 0) \qquad (23)$$

(ρ_W is the density of meltwater, Z_B is the bed elevation, and ϕ represents any additional water pressure associated with water storage). Meier and Post (1987) added a second component to the bed elevation term to account for any differences in density between meltwater, ρ_W, and the proglacial water body, ρ'_W:

$$P_W = [\rho_W g Z_B + (\rho'_W - \rho_W) g D_W] + \phi \qquad (23a)$$

The bed elevation term is easily calculated to yield a maximum value for the effective pressure in models of calving glaciers (e.g. Vieli et al., 2001). Calculated longitudinal strain rates depend sensitively on the rate at which ϕ increases upglacier, and the highest stretching and dynamic thinning rates occur when $\phi = 0$ (Fig. 13). Although unrealistic, this case is commonly assumed in numerical modeling studies (e.g. Vieli et al., 2001; Nick et al., in press). The ϕ term can be calculated explicitly (e.g. Flowers and Clarke, 2002), or derived from specified piezometric gradients (e.g. Benn et al., in press). In all cases, however, velocities and longitudinal strain rates increase rapidly as ice approaches flotation.

This has two important implications, which can account for much of the observed dynamic behavior of calving glaciers. First, *spatial* gradients in ice thickness relative to water depth result in increased sliding velocities and longitudinal strain rates (Meier and Post, 1987; Fig. 14). The high longitudinal strain rates observed near the termini of tidewater glaciers (0.1 to 0.8 yr^{-1} at Columbia Glacier, Venteris et al., 1997; 2 to 5 yr^{-1} at Le Conte Glacier, O'Neel et al., 2001) appear to be largely attributable to this process. High stretching rates near glacier termini will lead
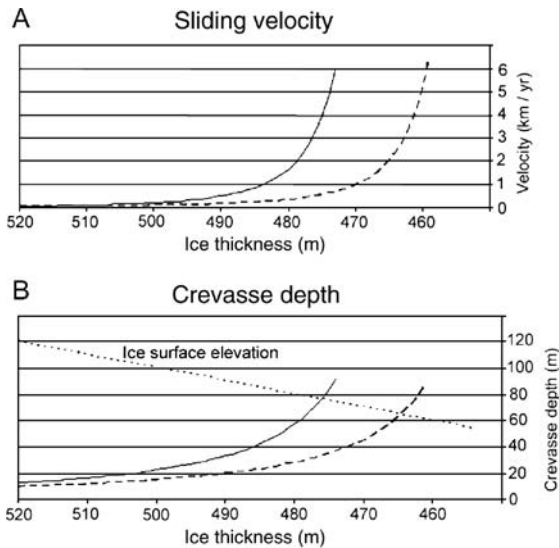
Fig. 14. A) Velocity gradients modelled using Eq. (22) and ice geometry and water depth representative of Columbia Glacier in 1988, for proglacial water densities of 1000 kg m^{-3} ('freshwater': dashed line) and 1030 kg m^{-3} ('salt water': solid line). B) Modelled crevasse depths. The terminus is assumed to be located where crevasse depth equals the ice surface elevation (dotted line), and the calving rate equal to the velocity at that point. For salt water conditions, the terminal ice cliff is higher, and the calving rate greater than the freshwater case. From Benn et al. (in press).

to deeper crevasses, so flow acceleration resulting from loss of basal drag will encourage calving.

Second, *temporal* reductions in ice thickness relative to water depth will result in flow acceleration and increasing longitudinal strain rates through time. Pritchard and Vaughan (in press) have presented convincing arguments that this mechanism accounts for an observed 12% increase in speed of glaciers throughout the Antarctic Peninsula between 1992 and 2005, and loss of basal drag consequent on glacier thinning may prove to be the principal reason for flow acceleration in many other regions. Furthermore, positive feedbacks between thinning and longitudinal stretching can explain how thickness changes, flow acceleration, and calving retreat form a self-reinforcing cycle that can amplify glacier response to an initial forcing (Vieli et al., 2001; Benn et al., in press). For constant-volume deformation in two dimensions, longitudinal stretching results in thinning in the vertical direction. Therefore, an initial thinning resulting from increased surface melting will lead to flow acceleration and longitudinal stretching, which will lead to further thinning, and so on (Fig. 15). Because crevasse depths also increase with longitudinal stretching (Section 3.3), this feedback will also increase calving losses and will trigger terminus retreat when increased calving losses outweigh the effects of flow acceleration.

Van der Veen (2002) has shown that glacier velocities calculated from Eqs. (22) and (23) are greater for tidewater than freshwater-calving glaciers. The effect is quite large, because the density difference between ice and salt water is significantly greater than that between ice and fresh water, such that its impact on basal effective pressure and sliding speed is correspondingly larger. The same is true for longitudinal strain rates (Benn et al., in press). The relationship between ice velocity and calving rate (Eq. (1)) means that, for any given combination of ice thickness and water depth, tidewater glaciers will experience greater calving losses than freshwater-calving glaciers (Fig. 14).

Although Budd-type sliding laws can be used to explain many aspects of the behavior of calving glaciers, they have important limitations. In particular, according to Eq. (22) U_B tends to infinity as P_E tends to zero. In glacier models, this unphysical behavior can be avoided using various numerical 'fixes', such as imposing an arbitrary minimum basal effective pressure (e.g. Nick et al., in press) or cutting off the glacier terminus before flotation occurs (Vieli et al. (2001). In Nature, runaway glacier acceleration is prevented because flow is impeded by other resisting stresses. The existence of such stresses is essential for the formation of ice shelves, so the role of other stresses in controlling ice flow must be considered in any comprehensive model of calving glacier dynamics.
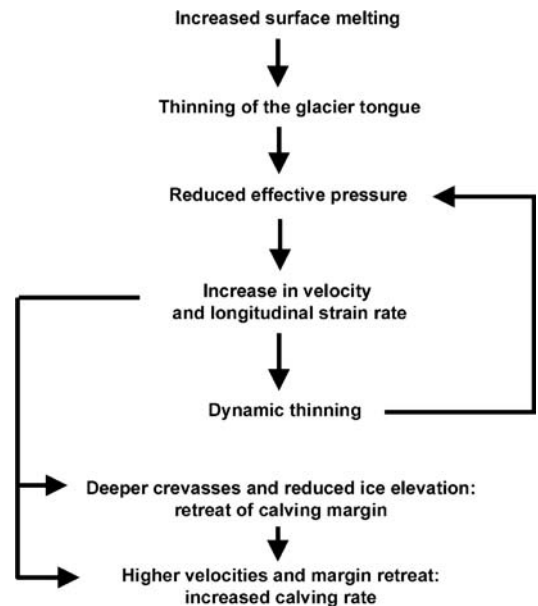

Fig. 15. Relationships between thinning, acceleration and calving retreat, resulting from effective pressure-dependent basal motion and the influence of longitudinal strain rate on dynamic thinning and first-order calving.

5.3. Lateral drag

On outlet glaciers, ice streams and ice shelves, driving stresses are also opposed by drag at the margins (e.g. Echelmeyer et al., 1994). Force balance analyses have shown that the proportion of driving stress supported by lateral drag varies considerably in space and time. For example, for Whillans Ice Stream (formerly Ice Stream B), Whillans and Van der Veen (1997) found that basal drag is minimal over most of the bed, and that almost all resistance to the driving stress is provided by lateral drag. In contrast, inverse modeling of Pine Island Glacier, Antarctica, by Payne et al. (2004) indicated that resistance from lateral drag is similar to that from basal drag along most of the glacier, except for a 50 km wide zone upglacier from the grounding line and another in the upper reaches of the glacier, where basal drag is very high. Reconstructions of the force balance of the retreating tidewater Columbia Glacier by O'Neel et al. (2005) indicate that lateral drag is generally less than basal drag, but becomes increasingly important during periods of rapid retreat.

Where lateral drag provides a significant proportion of resistance to flow, ice velocities will be poorly predicted by sliding laws such as Eq. (22). The effects of lateral drag on patterns of ice flow have been modeled by Raymond (1996) and Van der Veen (1999a,b). Both models assume that velocities are controlled by strain of ice in the x–y plane, and calculate flow speeds by integrating the flow law across the glacier half-width, W. A simple solution, analogous to that for the surface velocity resulting from ice creep, can be obtained by assuming that the flow law parameters A and n are constant and that the shear stress varies linearly across-glacier from maxima at the margins to zero at the centreline. For a rectangular cross section, the relationship between shear stress at the margin τ_S and driving stress τ_D is given by:

$$\tau_D = \frac{W}{H} \tau_S \tag{24}$$

so the velocity at the centreline U_{CR}, is:

$$U_{CR} = \frac{2A}{n+1} \left(\frac{\tau_D}{H}\right)^n W^{n+1}. \tag{25}$$

The definition of driving stress (Eq. (20)) means that the term inside the brackets equals $\rho_I g \partial h / \partial x$. Thus, according to Eq. (25), centreline velocity is independent of ice thickness and effective pressure, but is proportional to the third power of the ice surface gradient and the fourth power of the flow-unit width (taking $n = 3$). In this case, therefore, velocity will not tend to increase as ice thickness decreases, so that flow acceleration will not necessarily occur when ice tends towards flotation.

On the other hand, the very strong dependence of velocity on half-width explains the widely-observed tendency for calving glacier margins to be located at widenings in fjords or other embayments (e.g. Mann, 1986; Porter, 1989; Warren, 1991). Even small increases in width will result in large increases in velocity, so that longitudinal strain rates will tend to be high at such localities. The crevasse depth calving criterion (Section 4.6), predicts that the calving margin will be located where longitudinal strain rates are high enough to allow crevasses to penetrate to the waterline, so the glacier margin is most likely to be located where $\partial W / \partial x$ is large and h is small. Flow divergence at flow-unit widenings will reduce h, so this will further increase the likelihood that the crevasse depth criterion is met. Conversely, fjord narrowings will result in reductions in velocity and longitudinal compression, encouraging glacier terminus stability.

Inverse modelling of the velocity distribution of the pre-collapse Larsen B ice shelf by Vieli et al. (2006) clearly shows that the assumptions underlying Eq. (25) are over simplified. In particular, their modelling results demonstrate that the flow-law parameters A and n exhibit substantial spatial variations depending on the location and strain history of the ice, with ice shelf margins displaying pronounced softening relative to central, low-strain regions. Strain-softening at ice shelf or stream margins can occur as the result of extensive crevassing, ice-crystal fabric development or strain heating (increasing the Arrhenius parameter A), although strain-hardening has also been reported at some localities (Harrison et al., 1998). Although altered rheology at ice shelf or stream margins will affect the absolute values of ice velocity, the conclusion that ice flow is strongly dependent on channel width but independent of ice thickness appears to be robust.

5.4. Longitudinal stress gradients

Longitudinal stress gradients have long been considered a potentially significant factor in the stability of tidewater glaciers and ice shelves. At a vertical terminal face of a calving glacier, the outward-directed cryostatic pressure is greater than the backward-directed hydrostatic pressure, as noted in Section 3.4. For equilibrium, viscous stretching is required to balance this gradient in longitudinal stress. The same situation applies at the point of attachment between a grounded glacier and a free-floating, unconfined ice shelf (Weertman, 1957; Dupont and Alley, 2005). If, however, there are additional forces resisting flow of the ice shelf, such as drag at the shelf margins or at localized grounded zones, this
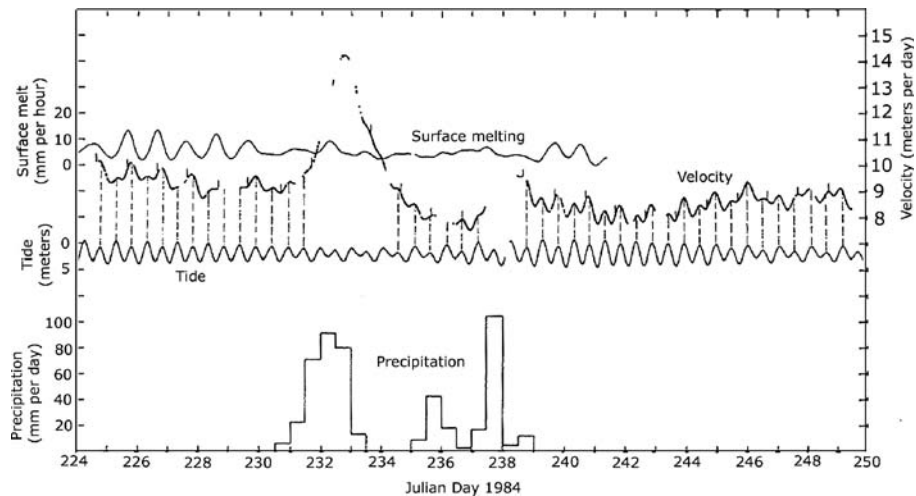
Fig. 16. Velocity, surface ablation, tide and precipitation, Columbia Glacier, 1984. The tidal data are inverted to highlight the close relationship between tide and velocity. From Krimmel and Vaughn (1987).

can partially or wholly offset the imbalance between cryostatic and hydrostatic pressures at the point of attachment. The additional backward-acting pressure is known as *backstress*. Van der Veen (1997) usefully defined the backstress on the grounded part of a calving glacier as the effects of non-local lateral and basal drag transmitted upglacier via longitudinal stresses. Backstress on calving glaciers can also occur as a result of obstructions to flow, such as fjord narrowings, grounding-line fans and terminal moraines.

The role of longitudinal stresses in controlling the flow of tidewater glaciers is clearly demonstrated by the relationship between tidal cycles and sliding speed (Fig. 16). Strong semidiurnal velocity cycles have been recorded in the terminal zones of Columbia Glacier (Meier and Post, 1987; Walters and Dunlap, 1987) and LeConte Glacier (O'Neel et al., 2001), in which velocity maxima coincide with low tide. The effect is quite large. At Columbia Glacier, a 1% variation in water depth at the terminus is associated with a 4% variation in speed, whereas at LeConte Glacier, a 1.5% variation in water depth causes a 5.5% variation in speed. This pattern reflects the time-varying longitudinal force balance at the terminus, with maximum backward-acting hydrostatic pressure at high tide. The effect decays upglacier, with a damping length (i.e. decay to $1/e$ of the peak value) of 2 km at Columbia and 0.5 km at Le Conte, a contrast that reflects the different magnitude of longitudinal stress gradients at the two glaciers (O'Neel et al., 2001). Interestingly, the relationship between water depth and flow speed at these glaciers is the opposite of that implied by Budd-type sliding laws (Section 5.2), probably because effective pressure is already so low near the glacier

termini that the longitudinal stress effect strongly outweighs any hydrostatic effect on basal drag. The patterns observed at Columbia and LeConte glaciers also contrast with the 'stick-slip' behavior of Whillans Ice Stream, which is attributable to tidally-modulated storage and release of elastic strain in basal till (Bindschadler et al., 2003).

Several authors have argued that longer-term changes in backstress can have a major impact on ice velocities. For example, Meier and Post (1987) suggested that the dramatic speed-up of Columbia Glacier in 1982 was partially in response to the release of backstress when the glacier retreated back from its terminal moraine. In contrast, Whillans and Venteris (1997) and Venteris et al. (1997) have argued that the behavior of Columbia Glacier since the onset of retreat is inconsistent with this interpretation, and that longitudinal stress gradients have had only a small effect on the evolving force balance of the glacier. A more rigorous force balance analysis of Columbia Glacier, however, has shown that longitudinal stress gradients locally play a very important role in opposing the driving stress, particularly upglacier of trough narrowings (O'Neel et al., 2005). These authors concluded that flow acceleration is indeed likely to occur when the glacier retreats from such 'pinning points'. Similarly, Johnson et al. (2004) attributed the recent doubling in the speed of Jakobshavns Isbrae to the disintegration of the floating part of the glacier tongue, which was formerly laterally constrained by a narrowing of Jakobshavn Isfjord. In this case, the floating ice was rheologically complex, consisting in part of highly fractured ice which 'jammed' in the constriction. Rheological differences aside, this appears to be similar

to the Columbia Glacier case, in which the effects of lateral constraint are transmitted upglacier by longitudinal stresses, and the removal of the constraint results in flow acceleration. Loss of laterally-confined ice shelves can also result in reduced backstress and flow acceleration, as has been observed in the Antarctic Peninsula, where collapse of the northern parts of the Larsen Ice Shelves was followed by acceleration of tributary glaciers (De Angelis and Skvarca, 2003; Rignot et al., 2004). It should be noted, however, that loss of backstress may not be the sole cause of this acceleration, as glaciers throughout the Antarctic Peninsula experienced increases in speed over this time interval (Pritchard and Vaughan, in press).

Reduction of backstress following the removal of ice shelves has received a great deal of attention as a possible trigger for rapid ice sheet deglaciation and consequent sea-level rise (e.g. Thomas and Bentley, 1978, Thomas et al., 1979; Hughes, 1986, 1992, 1998). It has been argued that, where ice sheets are grounded below sea level, ice shelves provide an essential 'buffer' between the continental ice and the ocean, and that ice shelf removal could initiate flow acceleration and 'drawdown' of the inland ice. One of the most prominent champions of this scenario has been Hughes (1986, 1998) who has argued that both the Greenland and West Antarctic ice sheets are vulnerable to rapid 'draw-down' and collapse by a mechanism he called the 'Jakobshavn effect'. His numerical model of this process, however, is built on the premise that the transition from sheet flow to ice-shelf flow is mediated solely by longitudinal stress gradients, and that longitudinal stresses 'pull' ice out of the interior. This formulation is at odds with detailed analyses of modern ice streams, which indicate that shifts between basal and lateral drag are more important than longitudinal stress gradients in modulating sheet-shelf transitions (Van der Veen and Whillans, 1996). Recent modelling of ice shelf buttressing effects support this latter view, and there is currently no evidence to support the idea that longitudinal stresses can sustain irreversible 'draw-down' (Payne et al., 2004; Dupont and Alley, 2005; Hindmarsh, 2006). Instead, these authors found that longitudinal stresses play an important but transient role in modulating shifts in resisting stresses, but that new equilibria are attained following imposed changes.

5.5. Representing calving glacier dynamics in ice sheet models

From the foregoing, it is clear that longitudinal strain rates (which control first-order calving processes as defined in Section 4.5) are functions of spatial variations in basal drag, lateral drag, longitudinal stress, or any combination of the three. Numerical models incorporating all sources of resistance to flow are now available, and can be used to explore the flow response of ice streams and ice shelves to imposed perturbations (e.g. Payne et al., 2004; Hindmarsh, 2006). Physically-based 'calving laws', such as the crevasse-depth calving criterion (Section 4.6), could be included in such models, as a means of evolving terminus positions and calculating calving rates. High-order flow models, however, are computationally expensive and as yet are impractical for representing ice margin evolution on the range of spatial and temporal scales relevant for ice sheets. For many applications, simpler approaches are required, in which some stress components are neglected and certain physical processes are parameterized using simple functions. One common strategy is to assume that the driving stress is entirely balanced by basal drag in grounded parts of the ice sheet (sheet flow), and by lateral drag and/or longitudinal stress gradients in the floating parts (shelf flow; Van der Veen and Payne, 2004). Model discontinuities at the grounding line (where one set of model assumptions must be replaced by another) bedevil this approach, making it difficult to obtain realistic solutions for velocity when the ice is near flotation. For the same reason, this approach is unsuitable for predicting calving margin positions (and therefore calving rates) from longitudinal velocity gradients and crevasse depths.

An alternative approach is to assume that the driving stress in the grounded part of the model domain is opposed by basal drag plus either longitudinal stress gradients or lateral drag. Since driving stress can be balanced by another source of resistance if basal drag vanishes, the flow of grounded and floating ice can be modeled within a single framework, avoiding the discontinuity problems of sheet flow models while retaining computational simplicity. A number of reduced force-balance velocity functions have been proposed. For example, in a model intercomparison exercise, Vieli and Payne (2005) modelled the transition between ice stream and ice shelf flow using a velocity function with only basal drag and longitudinal stress gradient terms:

$$2\frac{\partial}{\partial x}Hv\frac{\partial U}{\partial x}-\beta^2 U_{\mathrm{B}} = \rho_{\mathrm{I}}gH\frac{\partial h}{\partial x} \qquad (26)$$

where v is the effective viscosity and β is a variable friction coefficient. When $\beta=0$, this expression reduces to that for a free-floating ice shelf spreading in the x-direction only.

Given the importance of width variations in determining glacier velocity and the position of calving margins

(Section 5.3), it is important that a general velocity function for calving glaciers should include the effects of lateral drag. Simple velocity functions with basal and lateral drag terms have been proposed by Van der Veen and Whillans (1996) and Raymond (1996). Benn et al. (in press) derived a dimensional form of Raymond's (1996) dimensionless velocity function. They scaled basal drag to the driving stress and basal water pressure, and used the resulting function to modify the stress term in Eq. (25). Basal drag was assumed to be zero when $P_W = P_I$ and equal to the driving stress when $P_W = 0$. The variation of τ_D with P_W can be varied between these end points using a tuning parameter C:

$$\tau_B = \left(1 - \frac{P_W}{P_I}\right)^C \tau_D \qquad (27)$$

allowing a wide spectrum of possible relationships to be represented. Subglacial water pressure, P_W, is obtained from Eq. (23). Combining Eqs. (25) and (27) yields an expression for the centreline velocity:

$$U_B = \frac{2A}{n+1}\left(\frac{\tau_D - \tau_B}{H}\right)^n W^{n+1} \qquad (28)$$

This formulation implicitly assumes that the glacier cross section is rectangular, basal drag is constant across the bed, and longitudinal stress gradients are negligible in controlling ice flow. The latter simplification may be justifiable in many cases (Van der Veen, 1999b), although there may be important exceptions, such as when perturbed glacier systems are far from equilibrium (see Payne et al., 2004; Dupont and Alley, 2005; O'Neel et al., 2005; Hindmarsh, 2006). Despite these simplify-
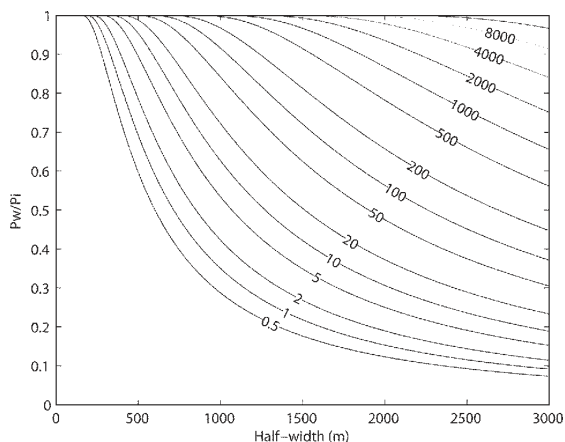

Fig. 17. Centreline velocities as a function of P_W/P_I and half-width W, calculated from Eq. (28). The example shown $\tau_D = 95$ kPa, $H = 480$ m, $C = 0.22$ (values representative of the terminal zone of Columbia Glacier in 1988).

ing assumptions, however, good matches are found between observed velocities and those predicted from Eq. (28) using known values of τ_D, H, W and Z_B. In the cases examined to date, the best matches are obtained when $C = 0.2$ to 0.3, and the water pressure component ϕ (Eq. (24)) increases upglacier (Benn et al., in press). The behavior of Eq. (28) is illustrated in Fig. 17, which shows velocities calculated for a range of glacier half-widths and $0 \leq P_W/P_I \leq 1$, for specified ice thickness and surface slope. The plot highlights the non-linear dependence of velocity on subglacial water pressure and channel width, and shows that Eq. (27) exhibits features of a Budd-type sliding law while parameterising the restraining influence of lateral drag. A crucial difference between Eq. (27) and Budd-type sliding laws, however, is that the former predicts finite velocities when $P_W = P_I$. This means that calving will not necessarily occur as the glacier approaches flotation, and it is possible for an ice shelf to form if conditions permit.

By coupling Eq. (28) with the crevasse-depth calving criterion (Eq. (18)), it is possible to model ice velocities and the position of the calving margin, and thus, calving rates. Longitudinal strain rates derived from Eq. (28) depend on the spatial scales over which P_W and W are varied. If either basal effective pressure decreases, or channel width increases over relatively short distances, velocities will increase rapidly downglacier, increasing the likelihood that longitudinal strain rates will be high enough to allow deep crevasses to form, and for calving to occur while the glacier is still grounded. In contrast, where basal effective pressure falls over a long spatial scale, and channel width does not increase significantly, ice may thin past the flotation thickness without major increases in velocity. In this case, longitudinal strain rates in the vicinity of the grounding line may be insufficient for crevasses to penetrate to the waterline, allowing an ice shelf to form (Fig. 18). If water-filled crevasses are prescribed (simulating the effect of surface melting), the ice shelf collapses and the glacier retreats past the grounding line.

When coupled with the crevasse-depth calving criterion, Eq. (28) also exhibits the same ice thickness — velocity feedback described in Section 5.2. Where basal drag provides a significant proportion of the resistance to flow, imposed thinning results in flow acceleration and increased longitudinal strain rates, leading to further dynamic thinning and ice front retreat (Fig. 15). Despite its simplicity, therefore, this model exhibits many important aspects of the observed dynamic behavior of calving glaciers, and can be used to model both grounded and floating ice fronts within a single framework. As currently formulated, this model neglects longitudinal
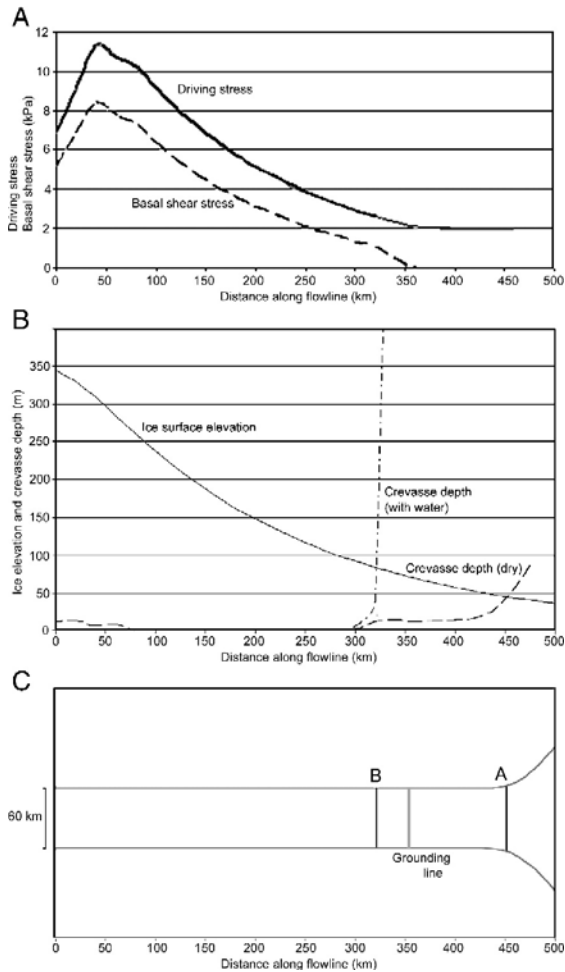
Fig. 18. Modelled stresses, crevasse depths and terminus position for an idealised outlet glacier of constant half-width of 30 km discharging into a widening fjord. (A) Driving stress and basal drag. Basal drag vanishes at the grounding line. (B) Prescribed ice surface elevation and modelled crevasse depths for dry and water-filled crevasses. (C) Plan view of outlet glacier geometry, showing position of the grounding line and the ice margin for the two crevasse scenarios. An ice shelf forms where surface crevasses are dry, and calving occurs at the fjord widening. Where water filled crevasses are prescribed on the lower glacier, the calving margin retreats to a grounded position.

stress gradients, and as noted in Section 5.4, this may mean that it cannot represent some significant phenomena. Longitudinal stress gradients arise as a result of spatial variations in basal and/or lateral drag, and the force imbalance at the terminal ice cliff. Explicit inclusion of longitudinal stress gradients in a general model could be achieved, but at the expense of a considerable increase in model complexity. Exploration of the importance of longitudinal stress gradients in the response to calving glaciers to imposed changes remains an important task.

An additional important issue is the asymmetry between the advance and retreat phases of calving glaciers. While glacier retreat is typically rapid, advance is generally very slow, and it has been argued that sediment shoals play a vital role in permitting the advance of calving glaciers into deep water (e.g. Post, 1975; Powell, 1991; Pelto and Warren, 1991; Hunter et al., 1996; Fischer and Powell, 1998). Sediment recycling processes allow subaqueous morainal banks to advance ahead of the glacier margin, providing a mobile 'pinning point' that effectively reduces water depth. This process has been modeled by Nick (2006) and Nick et al. (in press), who found that the late Holocene advance of Columbia Glacier could only be simulated if sediment cycling was included. Some representation of this process would therefore appear to be required in a fully comprehensive model of calving glacier dynamics.

6. Synthesis and conclusions

The importance of calving and related dynamic processes in the mass balance of past and present glaciers and ice sheets means that there is a pressing need for practical but robust 'calving laws' in prognostic ice sheet models. In this paper, we have argued that such 'laws' need to be firmly rooted in an understanding of physical processes, including both the fracture mechanics and dynamic aspects of the calving problem. While calving processes are both complex and diverse, for most purposes it is neither practical nor desirable to model individual calving events. Processes that are important locally can be ignored if the aim is to arrive at approximate, but realistic predictions of calving glacier behavior on regional scales. It is therefore necessary to approach the calving problem at an appropriate level of generalisation, to capture the essentials of the system without becoming mired in unnecessary detail.

A common feature of all calving events is the propagation of fractures. Because the stresses required for fracture growth can be generated in a wide variety of ways, it is useful to define a hierarchy of calving processes, to distinguish those that exert a fundamental control on the position of the ice margin from more localised processes responsible for individual calving events. We argue that the first-order control on calving is the strain rate arising from spatial variations in velocity (particularly sliding speed), which determines the location and depth of surface crevasses (Benn et al., in press). Where velocity gradients are large, deep crevasse penetration will encourage calving failure. Conversely, where velocity gradients are small, surface crevasses are less likely to trigger calving. Superimposed on this first-

order process are second-order processes that further erode the ice margin. These include: fracture propagation in response to local stress imbalances in the immediate vicinity of the glacier front (e.g. Reeh, 1968; Hughes, 1998; Hanson and Hooke, 2000, 2003); undercutting of the glacier terminus by melting at or below the waterline (e.g. Motyka et al., 2003a; Röhl, 2006); and bending at the junction between grounded and buoyant parts of an ice tongue. Calving of projecting, submerged 'ice feet' can be regarded as a third-order process, because it is paced by first-or second-order calving above the waterline (e.g. Motyka, 1997; O'Neel et al., in press).

This hierarchy does not imply that second-or third-order processes are necessarily less important than velocity gradients in determining calving rates, simply that lower order processes operate within the limits set by the large-scale dynamic setting of the glacier. Where high velocity gradients exist in the terminal zone of a glacier, first-order calving is likely to be the rate-limiting process. On the other hand, second-order processes may control the long-term calving rate where velocity gradients are small (such as on a glacier grounded in shallow water).

First-order calving can be effectively represented in glacier models using a crevasse-depth calving criterion (Benn et al., in press). Because a water-filled crevasse can penetrate downward without limit, full depth crevasses (rifts) will form where either (i) sufficient surface meltwater enters the crevasse, or (ii) the crevasse reaches sea-or lake level and water is allowed to flow in. In flowline models, the maximum possible position of the glacier margin can be defined as the point where crevasse depth equals the ice elevation above the proglacial water body. Three-dimensional glacier models must also take account of the lateral extent of crevasses and rifts. Crevasse depths can be calculated using the LEFM model of Van der Veen (1998a) or the simpler approach of Nye (1957). The computational simplicity of the latter makes it particularly suitable for incorporation within time-evolving glacier models.

The calving rate is defined as the ice velocity at the terminus minus the rate of change in glacier length. When the crevasse-depth calving criterion is adopted, modelling changes in terminus position and calving rates thus reduces to the problem of determining ice thickness, velocity distribution, and changes in thickness and velocity through time. In Nature, ice velocities are controlled by the magnitude of the driving stress, and the relative contributions of basal drag, lateral drag, and longitudinal stress gradients to resistance. Realistic solutions to the problem of modelling ice flow therefore depend critically on an appropriate choice of sliding law.

Recent models of calving glacier dynamics have employed Budd-type sliding laws, which implicitly assume that all resistance to flow is provided by basal drag (e.g. Vieli et al., 2000, 2001; Nick, 2006; Nick et al., in press). In such laws, the fundamental controls on velocity are the driving stress and basal effective pressure $(P_I - P_W)$. For calving glaciers where basal water flows towards the terminus, a minimum value of P_W is set by the elevation of the bed below lake or sea-level. This means that, for any given water depth, effective pressure falls as ice thickness decreases, so that ice velocity is sensitively dependent on changes in ice thickness in space and time. Such models can therefore replicate some important aspects of the behaviour of calving glaciers, including: downglacier increases in velocity as ice thins toward the waterline; high longitudinal strain rates and transverse crevasses close to glacier termini; flow acceleration in response to thinning through time; and the tendency for tidewater glaciers to stabilise in relatively shallow water (Vieli et al., 2000, 2001; Nick, 2006). Budd-type sliding laws, however, cannot be used to model floating glacier termini or ice shelves, because infinite velocities are predicted when effective pressure is zero. Height-above-buoyancy and crevasse-depth calving criteria can avoid such unphysical behavior by 'cutting off' the ice margin before flotation occurs, but of necessity Budd-type laws can only be applied to grounded glaciers unless some other source of resistance is included in the model.

On ice shelves and some ice streams, basal drag is negligible and a large proportion of resistance to flow is provided by drag at the lateral margins. In this case, velocity increases with ice surface slope and flow-unit width, but is independent of ice thickness (e.g. Van der Veen, 1999b). The dependence on width explains why tidewater glaciers and ice shelves commonly terminate at fjord or embayment widenings, where large velocity gradients encourage deep crevasses and calving. A sliding function developed by Benn et al. (in press) parameterises the effects of both basal and lateral drag. As in Budd-type laws, velocities are inversely proportional to basal effective pressure, but the inclusion of lateral drag means that velocities remain finite when basal drag vanishes. This means that the function can be used to model velocities for both grounded and floating ice. When coupled with the crevasse-depth calving criterion, this sliding function provides a simple and flexible means of representing calving and related dynamic processes in numerical ice sheet models.

The inclusion of longitudinal stress gradients in ice sheet models requires a considerable increase in model complexity. Although longitudinal stress gradients may be negligible in many cases (Van der Veen, 1999b), in

some circumstances they clearly exert a strong influence on glacier flow, especially where glacier systems are undergoing rapid change. Sudden reductions in backstress due to the removal of a confined ice shelf, for example, can dramatically alter the force balance near glacier termini, resulting in accelerating flow. Recent modelling work indicates that such effects are transient, and that following a reduction in backstress, glaciers will relax toward a new equilibrium state (Payne et al., 2004; Dupont and Alley, 2005). There is no evidence that longitudinal stress gradients can force sustained 'drawdown' and ice sheet collapse following ice shelf removal.

First-order calving, controlled by spatial gradients in velocity, can be used to explain a wide range of phenomena. Specifically:

(1) On the Columbia Glacier, short-term calving rate is inversely proportional to height above buoyancy (Sikonia, 1982). This is because velocity increases as basal drag is progressively reduced when the ice approaches flotation, increasing longitudinal strain rates and the depth of surface crevasses. In turn, this increases the likelihood of calving. The same principle provides a physical explanation for Van der Veen's (1996) height-above-buoyancy calving criterion. Importantly, though, the crevasse-depth calving criterion also permits ice to become fully buoyant, provided lateral drag provides sufficient resistance to flow.

(2) Correlations between longitudinal velocity gradients and calving rate are very weak. This is because velocity gradients are unrelated to the absolute value of the velocity. Longitudinal strain rates may control *where* calving occurs, but the calving *rate* is a function of ice velocity and rate of change in terminus position.

(3) Calving rates increase with water depth. The definition of calving rate means that there will be a strong correlation between calving rate and ice velocity, except during times of rapid terminus retreat (Van der Veen, 1996). Thus, faster glaciers will tend to have higher calving rates. The inverse relationship between effective pressure and basal drag means that glaciers flow faster when they enter deeper water.

(4) For a given water depth, calving rates tend to be greater for tidewater than freshwater-calving glaciers. This is due to the difference in density between salt-and fresh water, which controls the minimum water pressure beneath glacier termini (Van der Veen, 2002). Beneath a tidewater glacier, minimum water pressure is higher, so velocities, strain rates, and calving rates will all be higher than for a freshwater-calving glacier in the same depth of water.

(5) Calving margins tend to stabilise at topographic pinning points, i.e. where water is relatively shallow or at narrow points in fjords or embayments. This is because resistance from both basal and lateral drag is relatively high in such locations. It is difficult for ice to advance beyond pinning points because a downglacier decrease in basal and/or lateral resistance causes an increase in velocity and longitudinal stretching, encouraging calving.

(6) Tidewater glaciers in many parts of the world are undergoing thinning, acceleration and retreat. Thinning of the terminal zone of a tidewater glacier in response to increased surface ablation tends to reduce basal effective pressure and can trigger increases in sliding speed and longitudinal strain rates. If increased strain rates cause the calving margin to pull back from a pinning point, the process of thinning and flow acceleration can become self-sustaining, due to a positive feedback between thinning, falling effective pressure, ice velocity, longitudinal strain rate, and dynamic thinning (Vieli et al., 2001; Benn et al., in press). This mechanism applies where basal drag contributes significantly to the resisting stresses upglacier from the glacier terminus, because flow acceleration will occur when this drag is progressively lost as the ice approaches flotation. It does not apply where basal drag is insignificant near the grounding line, and most of the resistance to flow is provided by the glacier margins.

(7) The collapse of ice shelves fringing the Antarctic Peninsula occurred in response to increased surface melting. Water-filled crevasses can propagate downward without limit, so input of abundant meltwater allows pervasive rifting in areas where longitudinal stresses were hitherto insufficient to allow deep crevassing (Scambos et al., 2000).

It is unlikely that first-order calving is the sole mechanism operating at any one locality. Indeed, where longitudinal strain rates are small, calving may be dominated by lower-order processes. For example, where glacier ice terminates in relatively warm, vigorously circulating water, subaqueous melting is likely to be the dominant rate-controlling mechanism (Motyka et al., 2003a; Haresign and Warren, 2005). In such situations, a model based on the crevasse-depth calving criterion will overestimate the position of the calving margin, and underestimate the calving rate. Modelling subaqueous melt rates presents considerable challenges, and remains an important unsolved problem.

Finally, we can revisit the question raised in Section 1.1: what is the relationship between calving and glacier dynamics? Do calving losses play the role of 'master', triggering dynamic changes that propagate upglacier, or are they simply the 'slave', responding passively to dynamic processes? The great diversity of calving

processes and the wide range of factors that control glacier speed indicates that, in fact, framing the question in terms of 'master and slave' raises a false dichotomy. There is no simple unidirectional causal relationship between calving processes and glacier dynamics, both being part of a complex web of cause and effect with many feedbacks. Calving and the dynamics of calving glaciers can only be understood as inseparable parts of an intricately coupled system.

References

Alley, R.B., 1991. Sedimentary processes may cause fluctuations of tidewater glaciers. Annals of Glaciology 15, 119–124.

Alley, R.B., Dupont, T.K., Parizek, B.R., Anandakrishnan, S., 2005. Access of surface meltwater to beds of sub-freezing glaciers: preliminary insights. Annals of Glaciology 40, 8–14.

Bassis, J.N., Coleman, R., Fricker, H.A., Minster, J.B., 2005. Episodic propagation of a rift on the Amery Ice Shelf, East Antarctica. Geophysical Research Letters 32, L06502. doi:10.1029/2004GL022048.

Benn, D.I., Warren, C.R., 2002. Reply to the comments of J.P. Kenneally on "Buoyancy-driven lacustrine calving, Glaciar Nef, Chilean Patagonia" by C. Warren, D. Benn, V. Winchester and S. Harrison. Journal of Glaciology 48, 630.

Benn, D.I., Wiseman, S., Hands, K.A., 2001. Growth and drainage of supraglacial lakes on debris-mantled Ngozumpa Glacier, Khumbu Himal, Nepal. Journal of Glaciology 47, 626–638.

Benn, D.I., Hulton, N., Mottram, R., in press. 'Calving laws', 'sliding laws' and the stability of tidewater glaciers. Annals of Glaciology 46.

Bindschadler, R.R., 1980. The predicted behaviour of Griesgletscher and its possible threat to a nearby dam. Zeitschrift für Gletscherkunde und Glazialgeologie 16, 45–59.

Bindschadler, R.A., 1983. The importance of pressurized subglacial water in separation and sliding at the glacier bed. Journal of Glaciology 29, 3–19.

Bindschadler, R.A., Rasmussen, L.A., 1983. Finite difference model predictions of the drastic retreat of Columbia Glacier, Alaska. United States Geological Survey Professional Paper 1258-D.

Bindschadler, R.A., King, M.A., Alley, R.B., Anandakrishnan, S., Padman, L., 2003. Tidally-controlled stick-slip discharge of a West Antarctic ice stream. Science 301, 1087–1089.

Björnsson, H., Pálsson, F., Guðmundsson, S., 2001. Jokulsárlon at Breidamerkursandur, Vatnajökull, Iceland: 20th Century changes and future outlook. Jokull 50, 43101.

Boulton, G.S., Hindmarsh, R.C.A., 1987. Sediment deformation beneath glaciers: rheology and geological consequences. Journal of Geophysical Research 92, 9059–9082.

Boyce, E.S., Motyka, R.J., Truffer, M., in press. Flotation and retreat of a lake-calving terminus, Mendenhall Glacier, southeast Alaska. Journal of Glaciology 53.

Brown, C.S., Meier, M.F., Post, A., 1982. Calving speed of Alaska tidewater glaciers with applications to the Columbia Glacier, Alaska. U.S. Geological Survey Professional Paper, 1258-C. 13 pp.

Budd, W.F., Jenssen, D., 1987. Numerical modelling of the large-scale basal water flux under the West Antarctic Ice Sheet. In: Van der Veen, C.J., Oerlemans, J. (Eds.), Dynamics of the West Antarctic Ice Sheet. Kluwer, Dordrecht, pp. 293–320.

Budd, W.F., Keage, P.L., Blundy, N.A., 1979. Empirical studies of ice sliding. Journal of Glaciology 23, 157–170.

Chinn, T.J., 1996. New Zealand glacier responses to climate change of the past century. New Zealand Journal of Geology and Geophysics 39, 415–428.

Clarke, G.K.C., Marshall, S.J., Hillaire-Marcel, C., Bilodeau, G., Veiga-Pires, C., 1999. A glaciological perspective on Heinrich events. In: Clark, P.U., Webb, R.S., Keigwin, L.D. (Eds.), Mechanisms of global climate change at Millennial time scales. American Geophysical Union Monograph 112, pp. 243–262.

Cohen, D., Iverson, N.R., Hooyer, T.S., Fischer, U.H., Jackson, M., Moore, P.L., 2005. Debris-bed friction of hard-bedded glaciers. Journal of Geophysical Research-Earth Surface 110. doi:10.1029/2004JF000228.

Cutler, P.M., Mickelson, D.M., Colgan, P.M., MacAyeal, D.R., Parizek, B.R., 2001. Influence of the Great Lakes on the dynamics of the southern Laurentide ice sheet: numerical experiments. Geology 29, 1039–1042.

De Angelis, H., Skvarca, P., 2003. Glacier surge after ice shelf collapse. Science 299, 1560–1562.

Dowdeswell, J.A., 1989. On the nature of Svalbard icebergs. Journal of Glaciology 35, 224–234.

Dupont, T.K., Alley, R.B., 2005. Assessment of the importance of ice-shelf buttressing to ice-shelf flow. Geophysical Research Letters 32, L04503. doi:10.1029/2004GL022024.

Echelmeyer, K.A., Harrison, W., Larsen, C., Mitchell, J.E., 1994. The role of the margins in the dynamics of an active ice stream. Journal of Glaciology 40, 527–538.

Eijpen, K.J., Warren, C.R., Benn, D.I., 2003. Subaqueous melt rates at calving termini: a laboratory approach. Annals of Glaciology 36, 179–183.

Elsberg, D., Zirnheld, S., Echelmeyer, K., Trabant, D., Krimmel, R., 2003. The slow advance of a tidewater glacier: Hubbard Glacier, Alaska. Annals of Glaciology 36, 45–50.

Evans, H.E., 1984. Mechanisms of Creep Fracture. Elsevier, Amsterdam. 319 pp.

Fastook, J.L., Schmidt, W.F., 1982. Finite element analysis of calving from ice fronts. Annals of Glaciology 3, 103–106.

Fischer, M.P., Powell, R.D., 1998. A simple model for the influence of push-morainal banks on the calving and stability of glacial tidewater termini. Journal of Glaciology 44, 31–41.

Fischer, M.P., Alley, R.B., Engelder, T., 1995. Fracture toughness of ice and firn determined from the modified ring test. Journal of Glaciology 41, 383–394.

Flowers, G.E., Clarke, C.K.C., 2002. A multicomponent coupled model of glacier hydrology 1. Theory and synthetic examples. Journal of Geophysical Research 107 (B11). doi:10.1029/2001JB001122.

Fowler, A., 1987. Sliding with cavity formation. Journal of Glaciology 33, 255–267.

Funk, M., Röthlisberger, H., 1989. Forecasting the effects of a planned reservoir that will partially flood the tongue of Unteraargletscher in Switzerland. Annals of Glaciology 13, 76–80.

Hagen, J.O., Melvold, K., Pinglot, F., Dowdeswell, J.A., 2003. On the net mass balance of the glaciers and ice caps in Svalbard, Norwegian Arctic. Arctic, Antarctic and Alpine Research 35 (2), 264–270.

Hambrey, M.J., Muller, F., 1978. Structures and Ice deformation in the White Glacier, Axel Heiberg Island, North West Territories, Canada. Journal of Glaciology 20, 41–66.

Hanson, B., Hooke, R.LeB., 2000. Glacier calving: a numerical model of forces in the calving speed-water depth relation. Journal of Glaciology 46, 188–196.

Hanson, B.H., Hooke, R.LeB., 2003. Buckling rate and overhang development at a calving face. Journal of Glaciology 49, 578–586.

Haran, T., Bohlander, J., Scambos, T., Fahnestock, M. compilers. 2005. MODIS mosaic of Antarctica (MOA) image map. Boulder, CO, USA: National Snow and Ice Data Center. Digital media.

Haresign, E.C., 2004. Glacio-limnological Interactions at Lake-calving Glaciers. Unpublished PhD Thesis, University of St Andrews.

Haresign, E.C., Warren, C.R., 2005. Melt rates at calving termini: a study at Glaciar Léon, Chilean Patagonia. In: Harris, C., Murton, J.B. (Eds.), Cryospheric Systems: Glaciers and Permafrost. London, Geological Society Special Publication, vol. 242, pp. 99–110.

Harrison, W.D., Echelmeyer, K.A., Larsen, C.F., 1998. Measurement of temperature in a margin of Ice Stream B. Journal of Glaciology 44, 615–624.

Hindmarsh, R.C.A., 2006. The role of membrane-like stresses in determining the stability and sensitivity of the Antarctic Ice Sheets: back pressure and grounding line motion. Philosophical Transactions of the Royal Society of London. Series A 364, 1733–1767.

Holdsworth, G., 1969a. Primary transverse crevasses. Journal of Glaciology 8, 107–129.

Holdsworth, G., 1969b. Flexure of a floating ice tongue. Journal of Glaciology 8 (54), 385–397.

Holdsworth, G., 1973. Ice calving into proglacial Generator Lake, Baffin Island, North West Territories, Canada. Journal of Glaciology 12, 235–250.

Holdsworth, G., Glynn, J.E., 1981. A mechanism for the formation of large icebergs. Journal of Geophysical Research 86 (C4), 3210–3222.

Hooke, R.LeB., 2005. Principles of Glacier Mechanics, Second edition. Cambridge University Press. 429 pp.

Hooke, R.LeB., Laumann, T., Kennett, M.I., 1989. Austdalsbreen, Norway: expected reaction to a 40 m increase in water level in the lake into which the glacier calves. Cold Regions Science and Technology 17, 113–126.

Howarth, P.J., Price, R.J., 1969. The proglacial lake of Breiðamerkurjökull and Fjallsjökull, Iceland. Geographical Journal 135, 573–581.

Howat, I.M., Joughin, I., Tulaczyk, S., Gogineni, S., 2005. Rapid retreat and acceleration of Helheim Glacier, east Greenland. Geophysical Research Letters 32. doi:10.1029/2005GL024737.

Hughes, T.J., 1986. The Jakobshavns Effect. Geophysical Research Letters 13 (1), 46–48.

Hughes, T., 1989. Calving ice walls. Annals of Glaciology 12, 74–80.

Hughes, T.J., 1992. Theoretical calving rates from glaciers along ice walls grounded in water of variable depths. Journal of Glaciology 38 (129), 282–294.

Hughes, T., 1996. Can ice sheets trigger abrupt climatic change? Arctic and Alpine Research 28, 448–465.

Hughes, T.J., 1998. Ice Sheets. Oxford University Press, Oxford, p. 343.

Hughes, T., 2002. Calving bays. Quaternary Science Reviews 21, 267–282.

Hughes, T.J., Nakagawa, M., 1989. Bending shear: the rate-controlling mechanism for calving ice walls. Journal of Glaciology 35, 260–266.

Hulton, N.R., Purves, R.S., McCulloch, R.D., Sugden, D.E., Bentley, M.J., 2002. The Last Glacial Maximum and deglaciation in southern South America. Quaternary Science Reviews 21 (1–3), 233–241.

Hunter, L.E., Powell, R.D., 1998. Ice foot development at temperate tidewater margins in Alaska. Geophysical Research Letters 25, 1923–1926.

Hunter, L.E., Powell, R.D., Lawson, D.E., 1996. Morainal-bank sediment budgets and their influence on the stability of tidewater termini of valley glaciers entering Glacier Bay, Alaska, USA. Annals of Glaciology 22, 211–216.

Iken, A., 1977. Movement of a large ice mass before breaking off. Journal of Glaciology 19, 595–604.

Iken, A., 1981. The effect of subglacial water pressure on the sliding velocity of a glacier in an idealised numerical model. Journal of Glaciology 27, 407–421.

Iken, A., Bindschadler, R.A., 1986. Combined measurements of subglacial water pressure and surface velocity of Findelengletscher, Switzerland: conclusions about drainage system and sliding mechanism. Journal of Glaciology 32, 101–119.

Iken, A., Truffer, M., 1997. The relationship between subglacial water pressure and velocity of Findelengletscher, Switzerland, during its advance and retreat. Journal of Glaciology 43, 328–338.

Iverson, N.R., Hanson, B., Hooke, R.LeB., Jansson, P., 1995. Flow mechanism of glaciers on soft beds. Science 267, 80–81.

Jacobs, S.S., Helmer, H.H., Doake, C.S.M., Jenkins, A., Frolich, R.M., 1992. Melting of ice shelves and the mass balance of Antarctica. Journal of Glaciology 38, 375–387.

Jeffries, M.O., 1985. Ice shelf studies off northern Ellesmere Island, Spring 1983. Arctic 38, 174–177.

Johnson, J.V., Prescott, P.R., Hughes, T.J., 2004. Ice dynamics preceding catastrophic disintegration of the floating part of Jakobshavn Isbrae, Greenland. Journal of Glaciology 50, 492–504.

Josberger, E.G., Martin, S., 1981. A laboratory and theoretical study of the boundary layer adjacent to a vertical melting ice wall in salt water. Journal of Fluid Mechanics 111, 439–473.

Joughin, I., MacAyeal, D.R., 2005. Calving of large tabular icebergs from ice shelf rift systems. Geophysical Research Letters 32, L02501. doi:10.1029/2004GL020978.

Joughin, I., Waleed, A., Fahnestock, M., 2004. Large fluctuations in speed on Greenland's Jakobshavn Isbrae glacier. Nature 432, 608–610.

Kamb, B., Engelhardt, H., Fahnestock, M.A., Humphrey, N., Meier, M., Stone, D., 1994. Mechanical and hydrologic basis for the rapid motion of a large tidewater glacier. 2. Interpretation. Journal of Geophysical Research 99 (B8), 15,231–15,244.

Kavanaugh, J.L., Clarke, G.K.C., 2006. Discrimination of the flow law for subglacial sediment using in situ measurements and an interpretation model. Journal of Geophysical Research 111. doi:10.1029/2005JF000346.

Kehle, R.O., 1964. Deformation of the Ross Ice Shelf, Antarctica. Geological Society of America Bulletin 75, 259–286.

Kenneally, J.P., Hughes, T.J., 2002. The calving constraints on inception of Quaternary ice sheets. Quaternary International 95–96, 43–53.

Kenneally, J.P., Hughes, T.J., 2006. Calving giant icebergs: old principles, new applications. Antarctic Science 18 (3), 409–419.

Kennett, M., Laumann, T., Kjøllmoen, B., 1997. Predicted response of the calving glacier Svartisheibreen, Norway, and outbursts from it, to future changes in climate and lake level. Annals of Glaciology 24, 16–20.

Kirkbride, M.P., 1993. The temporal significance of transitions from melting to calving termini at glaciers in the central Southern Alps, New Zealand. The Holocene 3 (3), 232–240.

Kirkbride, M.P., Warren, C.R., 1997. Calving processes at a grounded ice cliff. Annals of Glaciology 24, 116–121.

Kirkbride, M.P., Warren, C.R., 1999. Tasman Glacier, New Zealand: Twentieth-century thinning and predicted calving retreat. Global and Planetary Change 22, 11–28.

Krabill, W., Frederick, E., Manizade, S., Martin, C., Sonntag, J., Swift, R., Thomas, R., Wright, W., Yungel, J., 1999. Rapid thinning of parts of the southern Greenland ice sheet. Science 283, 1522–1524.

Krimmel R.M., 1987. Columbia Glacier, Alaska: photogrammetry data set 1981–82 and 1984–85, USGS open file report, 87–219, U.S. Geological Survey, 104.

Krimmel, R.M., 2001. Photogrammetric data set, 1957–2000, and bathymetric measurements for Columbia Glacier, Alaska. USGS Water-Resources Investigations Report 01-4089 46 pp.

Krimmel, R.M., Vaughn, B.H., 1987. Columbia Glacier, Alaska; changes in velocity 1977–1986. Journal of Geophysical Research 92 (B9), 8961–8968.

Larour, E., Rignot, E., Aubry, D., 2004a. Modelling of rift propagation on Ronne Ice Shelf, Antarctica, and sensitivity to change. Geophysical Research Letters 31, L16404. doi:10.1029/2004GL020077.

Larour, E., Rignot, E., Aubry, D., 2004b. Processes involved in the propagation of rifts near Hemmen Ice Rise, Ronne Ice Shelf, Antarctica. Journal of Glaciology 50, 329–341.

Laumann, T., Wold, B., 1992. Reactions of a calving glacier to large changes in water level. Annals of Glaciology 16, 158–162.

Lazzara, M.A., Jezek, K.C., Scambos, T.A., MacAyeal, D.R., Van der Veen, C.J., 1999. On the recent calving of icebergs from the Ross Ice Shelf. Polar Geography 23, 201–212.

Lingle, C.S., Hughes, T., Kollmeyer, R.C., 1981. Tidal flexure of Jakobshavns Glacier, west Greenland. Journal of Geophysical Research 86 (B5), 3960–3968.

Lingle, C.S., Post, A., Herzfeld, U., Molnia, B., Krimmel, R.M., Roush, J.J., 1993. Bering Glacier surge and iceberg-calving mechanism at Vitus Lake, Alaska, USA. Journal of Glaciology 39, 722–727.

Lliboutry, L., 1968. General theory of subglacial cavitation and sliding of temperate glaciers. Journal of Glaciology 7 (49), 21–58.

MacAyeal, D.R., Scambos, T.A., Hulbe, C.L., Fahnestock, M.A., 2003. Catastrophic ice shelf break-up by an ice-shelf-fragment-capsize mechanism. Journal of Glaciology 49, 22–36.

MacAyeal, D.R., Okal, E.A., Aster, R.C., Bassis, J.N., Brunt, K.M., Cathles, L.M., Drucker, R., Fricker, H.A., Martin, S., Okal, M.H., Sergienko, O.V., Sponsler, M.P., Thom, J.E., 2006. Transoceanic wave propagation links iceberg calving margins of Antarctica with storms in tropics and Northern Hemisphere. Geophysical Research Letters 33. doi:10.1029/2006GL027235.

Mangerud, J., Jakobsson, M., Alexanderson, H., Astakhov, V., Clarke, G.K., Henriksen, M., Hjort, C., Krinner, G., Lunkka, J.P., Moller, P., Murray, A., Nikolskaya, O., Saarnisto, M., Svendsen, J.I., 2004. Ice-dammed lakes and rerouting of the drainage of northern Eurasia during the Last Glaciation. Quaternary Science Reviews 23 (11–13), 1313–1332.

Mann, D.H., 1986. Reliability of a fjord glacier's fluctuations for palaeoclimatic reconstructions. Quaternary Research 25, 10–24.

Meier, M.F., 1958. The mechanics of crevasse formation. IAHS Publication 46, 500–508.

Meier, M.F., 1994. Columbia Glacier during rapid retreat: interactions between glacier flow and iceberg calving dynamics. In: Reeh, N. (Ed.), Workshop on the Calving Rate of West Greenland Glaciers in Response to Climate Change. Danish Polar Center Report, Copenhagen, pp. 63–83.

Meier, M.F., 1997. The iceberg discharge process: observations and inferences drawn from the study of Columbia Glacier. In: Van der Veen, C.J. (Ed.), Calving Glaciers: Report of a Workshop, Feb. 28–March 2, 1997. Byrd Polar Research Centre Report No. 15. The Ohio State University, Columbus, Ohio, pp. 109–114.

Meier, M.F., Post, A., 1987. Fast tidewater glaciers. Journal of Geophysical Research 92 (B9), 9051–9058.

Meier, M.F., Lundstrom, S., Stone, D., Kamb, B., Engelhardt, H., Humphrey, N., Dunlap, W.W., Fahnestock, M., Krimmel, R.M., Wallters, R., 1994. Mechanical and hydrologic basis for the rapid motion of a large tidewater glacier. 1. Observations. Journal of Geophysical Research 99 (B8), 15,219–15,229.

Mercer, J.H., 1961. The response of fjord glaciers to changes in firn limit. Journal of Glaciology 10, 850–858.

Mercer, J.H., 1978. West Antarctic ice sheet and CO_2 greenhouse effect: a threat of disaster. Nature 271, 321–325.

Motyka, R.J., 1997. Deep-water calving at Le Conte Glacier, Southeast Alaska. In: Van der Veen, C.J. (Ed.), Calving Glaciers: Report of a Workshop, Feb. 28–March 2, 1997. Byrd Polar Research Centre Report No. 15. The Ohio State University, Columbus, Ohio, pp. 115–118.

Motyka, R.J., Hunter, L., Echelmeyer, K., Connor, C., 2003a. Submarine melting at the terminus of a temperate tidewater glacier, LeConte Glacier, Alaska, U.S.A. Annals of Glaciology 36, 57–65.

Motyka, R.J., O'Neel, S., Connor, C.L., Echelmeyer, K.A., 2003b. Twentieth century thinning of Mendenhall Glacier, Alaska, and its relationship to climate, lake calving and glacier runoff. Global and Planetary Change 35, 93–112.

Nansen, F., 1890. The First Crossing of Greenland. (English translation published by Birlinn Press, Edinburgh, 2002).

Nick, F.M., 2006. Modelling the behavior of tidewater glaciers. PhD thesis, University of Utrecht.

Nick, F.M., Oerlemans, J., 2006. Dynamics of tidewater glaciers: comparison of three models. Journal of Glaciology 52, 183–190.

Nick, F.M., Van der Veen, C.J., Oerlemans, J., in press. Controls on advance of tidewater glaciers: Results from numerical modelling applied to Columbia Glacier. Journal of Geophysical Research.

Nixon, W.A., Schulson, E.M., 1987. A micromechanical view of the fracture toughness of ice. Journal de Physique 48, 313–319.

Nye, J.F., 1951. The flow of glaciers and ice sheets as a problem in plasticity. Proceedings of the Royal Society of London A207 (1091), 554–572.

Nye, J.F., 1952. The mechanics of glacier flow. Journal of Glaciology 2, 82–93.

Nye, J.F., 1957. The distribution of stress and velocity in glaciers and ice sheets. Proceedings of the Royal Society of London. Series A 239, 113–133.

Nye, J.F., 1959. The deformation of a glacier below an ice fall. Journal of Glaciology 3, 386–408.

O'Neel, S., Echelmeyer, K.A., Motyka, R.J., 2001. Short-term flow dynamics of a retreating tidewater glacier: LeConte Glacier, Alaska, U.S.A. Journal of Glaciology 47, 567–578.

O'Neel, S., Echelmeyer, K.A., Motyka, R.J., 2003. Short-term variations in calving of a tidewater glacier: LeConte Glacier, Alaska, U.S.A. Journal of Glaciology 49, 587–598.

O'Neel, S., Pfeffer, W.T., Krimmel, R., Meier, M., 2005. Evolving force balance at Columbia Glacier, Alaska, during its rapid retreat. Journal of Geophysical Research 110, F03012. doi:10.1029/2005JF000292.

O'Neel, S., Marshall, H.P., McNamara, D.E., Pfeffer, W.T., in press. Detection and analysis of icequakes at Columbia Glacier, AK. Journal of Geophysical Research.

Paterson, W.S.B., 1994. The Physics of Glaciers, 3rd edition. Pergamon, Oxford. 480 pp.

Payne, A.J., Vieli, A., Shepherd, A.P., Wingham, D.J., Rignot, E., 2004. Recent dramatic thinning of largest west Antarctic ice stream triggered by oceans. Geophysical Research Letters 31. doi:10.1029/2004GL021284.

Pelto, M.S., Warren, C.R., 1991. Relationship between tidewater glacier calving velocity and water depth at the calving front. Annals of Glaciology 15, 115–118.

Petrenko, V.F., Whitworth, R.W., 1999. Physics of Ice. Oxford University Press, Oxford.

Petrovic, J.J., 2003. Mechanical properties of ice and snow. Journal of Materials Science 38, 1–6.

Porter, S.C., 1989. Late Holocene fluctuations of the fiord glacier system in Icy Bay, Alaska, U.S.A. Arctic and Alpine Research 21, 364–379.

Post, A., 1975. Preliminary Hydrography and Historic Terminal Changes of Columbia Glacier, Alaska. U.S.G.S. Hydrologic Investigations Atlas HA-559.

Post, A., 1997. Passive and active iceberg producing glaciers. In: Van der Veen (Ed.), Calving glaciers. Byrd Polar Research Center Report 15, pp. 121–135.

Post, A., Mayo, L.R., 1971. Glacier Dammed Lakes and Outburst Floods in Alaska. U.S.G.S. Hydrologic Investigations Atlas HA-455.

Powell, R.D., 1983. Glacial-marine sedimentation processes and lithofacies of temperate tidewater glaciers, Glacier Bay, Alaska. In: Molnia, B.F. (Ed.), Glacial Marine Sedimentation. Plenum Press, New York, pp. 185–232.

Powell, R.D., 1991. Grounding-line systems as second-order controls on fluctuations of tidewater termini of temperate glaciers. In: Anderson, J.B., Ashley, G.M. (Eds.), Glacial Marine Sedimentation: Palaeoclimatic Significance. Geological Society of America Special Paper, vol. 261, pp. 75–93.

Pralong, A., Funk, M., 2005. Dynamic damage model of crevasse opening and application to glacier calving. Journal of Geophysical Research 110. doi:10.1029/2004JB 003104.

Pralong, A., Funk, M., Lüthi, M.P., 2003. A description of crevasse formation using continuum damage mechanics. Annals of Glaciology 37, 77–82.

Pritchard, H.D., Vaughan, D.G., in press. Widespread acceleration of tidewater glaciers on the Antarctic Peninsula. Journal of Geophysical Research.

Purdie, J., Fitzharris, B., 1999. Processes and rates of ice loss at the terminus of Tasman Glacier, New Zealand. Global and Planetary Change 22, 79–91.

Raymond, C.F., 1996. Shear margins in glaciers and ice sheets. Journal of Glaciology 42 (140), 90–102.

Raymond, C.F., Harrison, W.D., 1987. Fit of ice motion models to observations from Variegated Glacier, Alaska. IAHS Publication 170: The Physical Basis of Ice Sheet Modelling, pp. 153–166.

Reeh, N., 1968. On the calving of ice from floating glaciers and ice shelves. Journal of Glaciology 7, 215–232.

Reeh, N., 1994. Calving from Greenland glaciers: observations, balance estimates of calving rates, calving laws. In: Reeh, N. (Ed.), Report on the workshop on the calving rate of West Greenland glaciers in response to climate change. Danish Polar Center, University of Copenhagen, pp. 85–102.

Reeh, N., Christensen, E.L., Mayer, C., Olesen, O.B., 2003. Tidal bending of glaciers: a linear viscoelastic approach. Annals of Glaciology 37, 83–89.

Rignot, E., Kanagaratnam, P., 2006. Changes in the velocity structure of the Greenland Ice Sheet. Science 311, 986–990.

Rignot, E., Rivera, A., Casassa, G., 2003. Contribution of the Patagonia Icefields of South America to sea level rise. Science 302 (5644), 434–437.

Rignot, E., Casassa, G., Gogineni, P., Krabill, W., Thomas, R., 2004. Accelerated ice discharge from the Antarctic Peninsula following the collapse of Larsen B ice shelf. Geophysical Research Letters 31. doi:10.1020/2004GL020697.

Rist, M.A., Murrell, S.A.F., 1994. Ice triaxial deformation and fracture. Journal of Glaciology 40, 305–318.

Rist, M.A., Sammonds, P.R., Murrell, S.A.F., Meredith, P.G., Oerter, H., Doake, C.S.M., 1996. Experimental fracture and mechanical properties of Antarctic ice: preliminary results. Annals of glaciology 23, 284–292.

Rist, M.A., Sammonds, P.R., Murrell, S.A.F., Meredith, P.G., Doake, C.S.M., Oerter, H., Matsuki, K., 1999. Experimental and theoretical fracture mechanics applied to Antarctic ice fracture and surface crevassing. Journal of Geophysical Research, Series B 104, 2973–2987.

Robin, G.d.Q., 1974. Depth of water filled crevasses that are closely spaced. Journal of Glaciology 13, 543.

Röhl, K., 2006. Thermo-erosional notch development at fresh-water-calving Tasman Glacier, New Zealand. Journal of Glaciology 52, 203–213.

Rott, H., Stuefer, M., Siegel, A., Skvarca, P., Eckstaller, A., 1998. Mass fluxes and dynamics of Moreno Glacier, Southern Patagonia Icefield. Geophysical Research Letters 25 (9), 1407–1410.

Roush, J.J., Lingle, C.S., Guritz, R.M., Fatland, D.R., Voronina, V.A., 2003. Surge-front propagation and velocities during the early-1993–95 surge of Bering Glacier, Alaska, U.S.A., from sequential SAR imagery. Annals of Glaciology 36, 37–44.

Russell-Head, D.S., 1980. The melting of free-drifting icebergs. Annals of Glaciology 1, 119–122.

Scambos, T.A., Hulbe, C., Fahnestock, M., Bohlander, J., 2000. The link between climate warming and break-up of ice shelves in the Antarctic Peninsula. Journal of Glaciology 46, 516–530.

Schulson, E.M., Hibler, W.D., 1991. The fracture of ice on scales large and small: Arctic leads and wing cracks. Journal of Glaciology 37, 319–322.

Schweizer, J., Iken, A., 1992. The role of bed separation and friction in sliding over an undeformable bed. Journal of Glaciology 38, 77–92.

Siegert, M.J., Dowdeswell, J.A., 1995. Modelling ice-sheet sensitivity to Late Weichselian environments in the Svalbard–Barents Sea Region. Journal of Quaternary Science 10, 33–43.

Siegert, M.J., Dowdeswell, J.A., 2004. Numerical reconstructions of the Eurasian Ice Sheet and climate during the Late Weichselian. Quaternary Science Reviews 23, 1273–1283.

Sikonia, W.G., 1982. Finite Element Glacier Dynamics Model Applied to Columbia Glacier, Alaska. United States Geological Survey Professional Paper 1258-B.

Skvarca, P., De Angelis, H., Naruse, R., Warren, C.R., Aniya, M., 2002. Calving rates in freshwater: new data from southern Patagonia. Annals of Glaciology 34, 379–384.

Smiraglia, C., Motta, M., Vassena, G., Diolaiuti, G., 2004. Dry calving processes at the ice cliff of an Antarctic local glacier: the study case of Strandline Glacier (Northern Victoria Land, Antarctica). Annals of Glaciology 39, 201–208.

Smith, R.A., 1976. The application of fracture mechanics to the problem of crevasse penetration. Journal of Glaciology 17, 223–228.

Smith, R.A., 1978. Iceberg cleaving and fracture mechanics—a preliminary survey. In: Husseiny, A.A. (Ed.), Iceberg Utilisation: Proceedings of the First International Conference and Workshops on Iceberg Utilisation for Fresh Water Production, Weather Modification and Other Applications. Pergamon Press, New York.

Stokes, C.R., Clark, C.D., 2004. Evolution of late glacial ice-marginal lakes on the northwestern Canadian Shield and their influence on the location of the Dubawnt Lake palaeo-ice stream. Palaeogeography, Palaeoclimatology, Palaeoecology 215, 155–171.

Stuefer, M., 1999. Investigations on mass balance and dynamics of Moreno Glacier based on field measurements and satellite

imagery. Unpublished PhD thesis, Leopold Franzens University, Innsbruck.

Teller, J.T., Kehew, A.E., 1994. Introduction to the Late Glacial history of large proglacial lakes and meltwater runoff along the Laurentide Ice Sheet. Quaternary Science Reviews 13, 795–799.

Theakstone, W.H., 1989. Further catastrophic breakup of a claving glacier: observations at Austerdalsisen, Svartisen, Norway, 1983-87. Geografiska Annaler 71A, 245–253.

Thomas, R.H., Bentley, C.R., 1978. A model for Holocene retreat of the West Antarctic Ice Sheet. Quaternary Research 10, 150–170.

Thomas, R.H., Sanderson, Y.J.O., Rose, K.E., 1979. Effect of climatic warming on the West Antarctic Ice Sheet. Nature 277, 355–358.

Thomas, R., Abdalati, W., Akins, T.L., Csatho, B.M., Frederick, E.B., Gogineni, S.P., Krabill, W.B., Manizade, S.S., Rignot, E.J., 2000. Substantial thinning of a major east Greenland outlet glacier. Geophysical Research Letters 27, 1291–1294.

Tulaczyk, S., Kamb, B., Engelhardt, H., 2000. Basal mechanics of Ice Stream B. I. Till mechanics. Journal of Geophysical Research 105, 463–481.

Van der Veen, C.J., 1996. Tidewater calving. Journal of Glaciology 42, 375–385.

Van der Veen, C.J., 1997. Backstress: what it is and how it affects glacier flow. In: Van der Veen, C.J. (Ed.), Calving Glaciers: Report of a Workshop, Feb. 28–March 2, 1997. Byrd Polar Research Centre Report No. 15. The Ohio State University, Columbus, Ohio, pp. 173–180.

Van der Veen, C.J., 1998a. Fracture mechanics approach to penetration of surface crevasses on glaciers. Cold Regions Science and Technology 27, 31–47.

Van der Veen, C.J., 1998b. Fracture mechanics approach to penetration of bottom crevasses on glaciers. Cold Regions Science and Technology 27, 213–223.

Van der Veen, C.J., 1999a. Crevasses on glaciers. Polar Geography 23, 213–245.

Van der Veen, C.J., 1999b. Fundamentals of Glacier Dynamics. Balkema, Rotterdam.

Van der Veen, C.J., 2002. Calving glaciers. Progress in Physical Geography 26, 96–122.

Van der Veen, C.J., Payne, A.J., 2004. Modelling land-ice dynamics. In: Bamber, J., Payne, A.J. (Eds.), Mass Balance of the Cryosphere. Cambridge University Press, pp. 169–225.

Van der Veen, C.J., Whillans, I.M., 1987. Force budget: I. Theory and numerical methods. Journal of Glaciology 35, 53–60.

Van der Veen, C.J., Whillans, I.M., 1996. Model experiments on the evolution and stability of ice streams. Annals of Glaciology 23, 129–137.

Vaughan, D.G., 1993. Relating the occurrence of crevasses to surface strain rates. Journal of Glaciology 39, 255–266.

Venteris, E.R., 1997. Evidence for bottom crevasse formation on Columbia Glacier, Alaska. In: Van der Veen, C.J. (Ed.), Calving Glaciers: Report of a Workshop, Feb. 28–March 2, 1997. Byrd Polar Research Centre Report No. 15. The Ohio State University, Columbus, Ohio, pp. 181–185.

Venteris, E.R., 1999. Rapid tidewater glacier retreat: a comparison between Columbia Glacier, Alaska and Patagonian calving glaciers. Global and Planetary Change 22, 131–138.

Venteris, E.R., Whillans, I.M., Van der Veen, C.J., 1997. Effect of extension rate on terminus position, Columbia Glacier, Alaska, USA. Annals of Glaciology 24, 49–53.

Vieli, A., Payne, A.J., 2005. Assessing the ability of numerical ice sheet models to simulate grounding line migration. Journal of Geophysical Research 110. doi:10.1029/2004JF000202.

Vieli, A., Funk, M., Blatter, H., 2000. Tidewater glaciers: frontal flow acceleration and basal sliding. Annals of Glaciology 31, 217–221.

Vieli, A., Funk, M., Blatter, H., 2001. Flow dynamics of tidewater glaciers: a numerical modelling approach. Journal of Glaciology 47, 595–606.

Vieli, A., Jania, J., Kolondra, L., 2002. The retreat of a tidewater glacier: observations and model calculations on Hansbreen, Spitsbergen. Journal of Glaciology 48, 592–600.

Vieli, A., Jania, J., Blatter, H., Funk, M., 2004. Short-term velocity variations on Hansbreen, a tidewater glacier in Spitsbergen. Journal of Glaciology 50, 389–398.

Vieli, A., Payne, A.J., Zhijun, D., Shephard, A., 2006. Numerical modelling and data assimilation of the Larsen B ice shelf, Antarctic Peninsula. Philosophical Transactions of the Royal Society 364, 1815–1839.

Vornberger, P.L., Whillans, I.M., 1990. Crevasse deformation and examples from Ice stream B, Antarctica. Journal of Glaciology 36, 3–10.

Walters, R.A., Dunlap, W.W., 1987. Analaysis of time series of glacier speed: Columbia Glacier, Alaska. Journal of Geophysical Research 92 (B9), 8969–8975.

Warren, C.R., 1991. Terminal environment, trough geometry, and recent fluctuations of West Greenland glaciers. Boreas 20, 1–15.

Warren, C.R., 1999. Calving speed in freshwater at Glaciar Ameghino, Patagonia. Zeitschrift für Gletscherkunde und Glazialgeologie 35, 21–34.

Warren, C.R., 1992. Iceberg calving and the glacioclimatic record. Progress in Physical Geography 16, 253–282.

Warren, C.R., Aniya, M., 1999. The calving glaciers of southern South America. Global and Planetary Change 22 (1–4), 59–77.

Warren, C.R., Kirkbride, M.P., 2003. Calving speed and climatic sensitivity of New Zealand lake-calving glaciers. Annals of Glaciology 36, 173–178.

Warren, C.R., Greene, D., Glasser, N.F., 1995a. Glaciar Upsala, Patagonia: rapid calving retreat in fresh water. Annals of Glaciology 21, 311–316.

Warren, C.R., Glasser, N.F., Harrison, S., Winchester, V., Kerr, A.R., Rivera, A., 1995b. Characteristics of tide-water calving at Glaciar San Rafael, Chile. Journal of Glaciology 41, 273–289.

Warren, C.R., Benn, D.I., Winchester, V., Harrison, S., 2001. Buoyancy-driven lacustrine calving, Glaciar Nef, Chilean Patagonia. Journal of Glaciology 47, 135–146.

Weber, L.J., Nixon, W.A., 1996. Fracture toughness of freshwater ice—Part I: Experimental technique and results. ASME Journal of Offshore Mechanics and Arctic Engineering 118, 135–140.

Weertman, J., 1957. Deformation of floating ice shelves. Journal of Glaciology 3, 38–42.

Weertman, J., 1973. Can a water filled crevasse reach the bottom surface of a glacier? IAHS Publication 95, 139–145.

Weiss, J., 2004. Subcritical crack propagation as a mechanism of crevasse formation and iceberg calving. Journal of Glaciology 50, 109–115.

Whillans, I.M., Van der Veen, C.J., 1997. The role of lateral drag in the dynamics of Ice Stream B, Antarctica. Journal of Glaciology 43, 231–237.

Whillans, I.M., Venteris, E.R., 1997. Backstress on Columbia Glacier. In: Van der Veen, C.J. (Ed.), Calving Glaciers: Report of a Workshop, Feb. 28–March 2, 1997. Byrd Polar Research Centre Report No. 15. The Ohio State University, Columbus, Ohio, pp. 187–194.

Whillans, I.M., Jackson, M., Tseng, Y.-H., 1993. Velocity pattern in a transect across Ice Stream B, Antarctica. Journal of Glaciology 39, 562–572.

Yamada, T., 1998. Glacier Lake and its outburst flood in the Nepal Himalaya. Data Center for Glacier Research, Monograph No. 1. Tokyo, Japan. 96 pp.

Zwally, H.J., Abdalati, W., Herring, T., Larson, K., Saba, J., Steffen, K., 2002. Surface melt-induced acceleration of Greenland Ice-sheet flow. Science 297, 218–222.

Zweck, C., Huybrechts, P., 2003. Modeling the marine extent of Northern Hemisphere ice sheets during the last glacial cycle. Annals of Glaciology 37, 173–180.